

**This item is the archived peer-reviewed author-version of:**

Laser-induced excitation mechanisms and phase transitions in spectrochemical analysis : review of the fundamentals

**Reference:**

Vanraes Patrick, Bogaerts Annemie.- Laser-induced excitation mechanisms and phase transitions in spectrochemical analysis : review of the fundamentals  
Spectrochimica acta: part B : atomic spectroscopy - ISSN 0584-8547 - 179(2021), 106091  
Full text (Publisher's DOI): <https://doi.org/10.1016/J.SAB.2021.106091>  
To cite this reference: <https://hdl.handle.net/10067/1768760151162165141>

# Laser-induced excitation mechanisms and phase transitions in spectrochemical analysis – review of the fundamentals

Patrick Vanraes<sup>1</sup>, Annemie Bogaerts<sup>1</sup>

<sup>1</sup>PLASMANT, Department of Chemistry, University of Antwerp, Universiteitsplein 1, 2610 Wilrijk-Antwerp, Belgium

## *Abstract*

Nowadays, lasers are commonly applied in spectrochemical analysis methods, for sampling, plasma formation or a combination of both. Despite the numerous investigations that have been performed on these applications, the underlying processes are still insufficiently understood. In order to fasten progress in the field and in honor of the lifework of professor Rick Russo, we here provide a brief overview of the fundamental mechanisms in laser-matter interaction as proposed in literature, and throw the spotlight on some aspects that have not received much attention yet. For an organized discussion, we choose laser ablation, laser desorption and the associated gaseous plasma formation as the central processes in this perspective article, based on a classification of the laser-based spectrochemical analysis techniques and the corresponding laser-matter interaction regimes. First, we put the looking glass over the excitation and thermalization mechanisms in the laser-irradiated condensed phase, for which we propose the so-called multi-plasma model. This novel model can be understood as an extension of the well-known two-temperature model, featuring multiple thermodynamic dimensions, each of which corresponds to a quasi-particle type. Next, the focus is placed on the mass transfer and ionization mechanisms, after which we shortly highlight the possible role of anisotropic and magnetic effects in the laser-excited material. We hope this perspective article motivates more fundamental research on laser-matter interaction, as a continuation of the lifework of Rick Russo.

## **TABLE OF CONTENTS**

### **1. INTRODUCTION**

### **2. LASERS IN SPECTROCHEMICAL ANALYSIS**

2.1 A classification of laser-based spectrochemical analysis technology – breaking down the principles

2.2 Laser parameters affecting ablation, breakdown and desorption – the authoritarian laser regimes

### **3. LASER-MATTER INTERACTION ACCORDING TO THE MULTI-PLASMA MODEL**

3.1 The laser-initiated excitation mechanisms – so excited that you just can't hide it

3.2 Thermalization mechanisms – relaxation therapy for materials

### **4. LASER SPUTTERING MECHANISMS**

4.1 Mass transfer and phase transitions – faster than greased lightning

4.2 Laser-induced ionization and the plasma sheath – where the debate gets truly charged

4.3 Anisotropy and magnetic effects – asking for directions

### **5. CONCLUSION**

#### **1. Introduction**

In the field of spectrochemical analysis, laser-based methods play an important role for the detection, identification and examination of both organic and inorganic materials. They generally have numerous benefits over alternative techniques, because they often require no sample preparation, no vacuum conditions and a minimal sample volume, while simultaneously enabling a rapid analysis turn-around time, depth and lateral resolution measurements, and chemical mapping with virtually no waste production. They are viable for practically all industries, including geochemistry [1, 2], archeology [1], mining, industrial processing, environmental [2, 3] and food safety [4], forensics [1, 5, 6] and biology [7, 8]. Examples of their application in scientific research can be found throughout the articles contributed to this special issue in honor of Richard (Rick) E. Russo. Professor Rick Russo more specifically devoted the greater part of his career to the different aspects of laser ablation for chemical analysis. Already early on, around 1995, his research focal point shifted from laser deposition of thin films to laser ablation as a sample introduction technique, for inductively coupled plasma mass spectrometry (LA-ICP-MS) or atomic emission spectrometry (LA-ICP-AES). About 10 years later, he included laser-induced breakdown spectroscopy (LIBS) in his work as a stand-alone diagnostic method, which evolved into a parallel research line with an equivalent importance from 2010 onwards. As Russo and his co-workers pointed out in [7], LIBS can even serve as a complementary technique to LA-ICP-MS, since it can detect elements like H, O, F, N and Cl, which are inaccessible or hard to measure with the latter technique.

As in most areas in science, the technological progress in such laser-based spectrochemical analytical methods has taken a head start on the fundamental understanding of the underlying processes. Yet, further advancement requires deeper insight. Rick Russo's work of the past three decades cannot be thought away from this equation, since it strongly focused on the fundamentals of laser ablation and LIBS. Still, much remains to be discovered about the initiation and evolution of these processes, as the scientific debate on them continues. In particular, a profound knowledge and insight in the elementary mechanisms behind the laser-induced excitation and relaxation processes, charging effects, plasma sheath, mass transfer and the transition into an ionized gas is still lacking [1, 9]. Despite the countless informative review papers published on laser-based atomic spectroscopy, most of them do not focus on the fundamentals and only a few of them dug deeper into a few specific basic aspects. Laser-induced phase transitions, for example, have mainly been discussed from a thermal standpoint, whereas non-thermal effects stayed more under the radar. Although several mechanisms have been proposed and investigated for the excitation, thermalization, mass transfer and ionization processes during laser-matter interaction, an accurate and structured description of the underlying physical principles is still lacking. Additionally, most current theories have not yet adopted several essential insights from neighboring domains, such as laser-induced periodic surface structures, plasma sheath physics, magnetohydrodynamics and quasi-particle formulations in condensed matter physics. Therefore, an overview and restructuring of the available knowledge is desirable and likely even a crucial requirement for faster progress in the field.

The present perspective article aims to provide such a concise overview and proposes new directions for future research. In order to structure the discussion on the fundamentals, the most important laser-matter interaction processes and regimes need to be identified. For this purpose, Section 2 classifies laser-based spectrochemical analysis technologies according to the role played by the laser, revealing laser ablation, LIBS and laser desorption ionization as the three main core principles. Next, the need is discussed for a further subclassification as a function of the laser fluence, pulse duration and wavelength, since a variation of these parameters induces different ablation, breakdown and

desorption regimes. Section 3 subsequently zeros in on the excitation and thermalization mechanisms during laser-matter interaction. To this end, we introduce the so-called multi-plasma model for electronically excited materials, based on non-equilibrium thermodynamics and quasi-particle physics. This model not only serves as a conceptual framework for scientists working on laser-excited matter in general, but also can be used as a theoretical toolbox and building platform for more extensive computational methods. Next, Section 4 considers the transition from the dense laser-excited matter into an ionized gas, with the spotlight on mass transfer, phase transitions, the origin of the gaseous ions and plasma sheath formation. We also shortly touch upon the anisotropic and magnetic effects in the laser-matter interaction. Finally, in the concluding Section 5, we summarize the existing theories and pave a road that we believe will lead to more profound insight and new discoveries in laser-based spectrochemical analysis methods. We thus aim to walk in Rick Russo's footsteps, towards a better understanding of the fundamental physics underlying the aforementioned technologies. Hence, we hope this work will not only be a worthy addition to the special issue in honor of Rick, but also that it can help researchers inside and outside the domain of laser-based spectrochemical analysis to obtain a more comprehensive view on laser-matter interaction in general.

## 2. Lasers in spectrochemical analysis

### 2.1 A classification of laser-based spectrochemical analysis technology – breaking down the principles

In order to have a structured discussion, we first need to identify the central aspects of laser-matter interaction for their application in spectrochemical analysis. For this purpose, we briefly map in the present section the role of lasers in established and proposed techniques. Next to LA-ICP-MS, LA-ICP-AES and LIBS, many other laser-based spectrochemical analysis methods have namely been developed (see Figure 1). One class of alternatives employ a different ionization process between the laser ablation stage and the spectrometer, such as atmospheric pressure chemical ionization (LA-APCI-MS) [10, 11], ambient desorption/ionization (LA-ADI-MS) [12], electrospray ionization (LA-ESI-MS) [13-16] or liquid sampling-atmospheric pressure glow discharge (LA-LS-APGD-MS) [17, 18]. The laser ablated particles can also be caught first into a liquid phase before further analysis, by extraction techniques as liquid vortex capture (LA-LVC-ESI-MS) [19] or a liquid microjunction surface sampling probe coupled to high-precision liquid chromatography (LA-LMJSSP-HPLC-ESI-MS) [20]. In all of these cascade systems, laser ablation simply serves as the initiating extraction method to transfer particles from the sample into the analysis instrument.

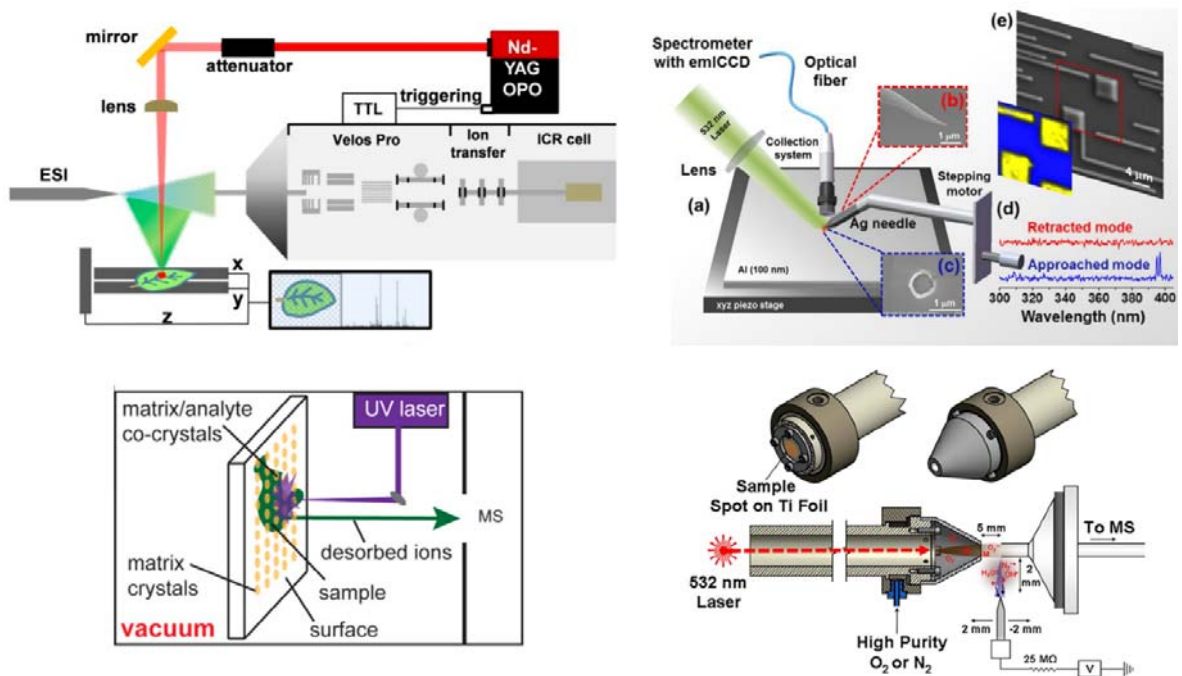


Figure 1. Examples of the four proposed categories of laser-based spectrochemical analysis technology, with (top left) LA-ESI-MS representing the methods applying laser ablation as a pure sampling technique, (top right) near-field enhanced LIBS to illustrate LIBS-based procedures, (bottom left) MALDI exemplifying the LDI group and (bottom right) LIAD as an indirect method. (top left) Reprinted with permission from [13]. Copyright (2019) American Chemical Society. (top right) Adapted from [21], Copyright (2018), with permission from Elsevier. (bottom left) Reprinted from [22], Copyright (2013), with permission from Elsevier. (bottom right) Adapted with permission from [23]. Copyright (2012) American Chemical Society.

It can, however, also simultaneously function as a plasma source, permitting the direct use of plasma diagnostics. Employing optical emission spectroscopy during laser ablation (LA-OES), for instance, in fact corresponds to LIBS. This core principle has led to another class of combined spectrochemical analysis techniques, which aim to optimize the laser-induced plasma features for a higher optical measurement sensitivity or resolution. As a straightforward option, a second laser pulse can enhance the plasma intensity and thus the optical signal, which has been concisely discussed in an earlier review by Babushok et al. [24]. An external high voltage source enables different ways to intensify the plasma as well, illustrated by laser ablation spark induced breakdown spectroscopy (LA-SIBS), where a laser pulse and a spark discharge are applied on the sample at the same location and moment [25]. If, on the other hand, the spatial measurement resolution needs to be refined, the laser can be combined with a sharp electrode, e.g. an AFM tip, hovering above the irradiated surface. This technique is known as tip-enhanced near-field laser ablation and has been investigated for diagnostic purposes in several contemporary articles [21, 26-29]. It should not be confused with so-called near-field optical laser ablation, where the laser beam is guided through a tapered optical fiber tip, such as one used for scanning near-field optical microscopy, also to obtain a higher spatial resolution [30].

These laser-based methods can be further optimized by modifying the surrounding sample conditions. Elemental fractionation may, for example, be reduced by injecting a reactive gas at the ablation site

during laser irradiation, which has been introduced by Hirata under the name of chemically assisted laser ablation (CLA) [31]. More specifically, he discovered a decreased Pb/U fractionation for zircon samples when Freon gas was introduced in the laser cell, and explained this effect with the production of volatile  $UF_6$  and thus less uranium redeposition. Obviously, the ablation process will also be highly influenced by a liquid environment. Underwater LIBS has gained significant recent interest due to the possibility of on-site spectrochemical analysis in marine archeology and more general ocean research [32-35]. In combination with electrodeposition, it also provides a promising strategy for metal ion detection in solutions [36-38].

Besides that, the extraction and ionization process may be improved by fine-tuning the laser features in order to match the sample. When the laser wavelength approaches a characteristic wavelength of the sample, such as a molecular absorption band, a larger amount of mass can be ejected at a lower fluence [39-42]. This forms the basic principle of resonant laser ablation or LIBS (RLIBS). A practically more complicated variant, called resonance-enhanced LIBS (RELIBS), applies two lasers, one of which initiates the ablation and the second one excites the ablated plume by means of the characteristic wavelength [39, 40, 43]. Both techniques display multiple benefits in analytical performance over classical LIBS, such as a similar or higher limit of detection with less sample damage [39-43], and a tunable selectivity to specific analytes [41, 44]. This makes them very closely related to soft laser desorption, also known under the more popular term of laser desorption ionization (LDI), which enables the extraction of intact molecular structures [5, 45]. Note that some texts on LDI define pure desorption as the direct and non-destructive transfer of a species from the condensed to the gaseous phase. For the remainder of this perspective article, however, we adopt a broader meaning for LDI, including all laser-based methods that promote molecular extraction under softer transport and ionization conditions.

Based on the most recent IUPAC nomenclature and a review by Kuzema [45, 46], LDI can be subdivided into direct (matrix-less), matrix-assisted (MALDI), surface-enhanced (SELDI) and surface-assisted (SALDI) laser desorption ionization, depending on the preparation of the sample. In MALDI, the analyte is first processed into a solid or liquid matrix that matches the laser wavelength for an optimal desorption. SELDI, on the other hand, replaces the matrix with a surface coating, which either enhances the laser desorption (surface enhanced neat desorption abbreviated as SEND), or selectively retains distinct protein or peptide types by means of their physicochemical properties or biochemical affinity (surface enhanced affinity capture, or SEAC) [45, 46]. The term SALDI often encapsulates different techniques using porous surfaces, nanoparticles, or nanostructured coatings that promote the laser desorption of macromolecules, although its demarcation varies throughout the scientific literature (see e.g. [5, 45, 46]). Direct matrix-less LDI, in contrast, mainly applies to small analyte molecules [45].

In addition to these plasma intensification and sample preparation procedures with appropriate wavelength-matching of the laser, advanced diagnostics allow a higher measurement sensitivity and selectivity of the generated plasma. When a second laser pulse is used as a probe for absorption or fluorescence spectroscopy, ground states of preselected plasma species can be accurately detected, which is impossible with classical optical emission spectroscopy. This principle in LIBS has earlier been reviewed by Cai et al. [47] and recently by Harilal et al. [1]. Russo and co-workers proposed an alternative adjustment of LIBS specifically for isotopic analysis, which he called laser ablation molecular isotopic spectrometry (LAMIS) [48]. This technique exploits isotope shifts in spectra of

molecular species either directly vaporized from a sample or formed by associative mechanisms in the laser ablation plume, to determine isotopic ratios of elements in the sample. A review on this topic is given in [49].

Last, but not least, a few techniques use lasers in a rather indirect manner for spectrochemical analysis. For instance, laser ablation enables surface scale layer removal or depth profiling for other analytical methods [50-53]. When a metal foil is irradiated with a laser at one side, the triangularly shaped generated shockwaves can cause molecules from a sample at the other side to be desorbed, a procedure called laser-induced acoustic desorption (LIAD) [9, 54]. This method serves as an alternative to more popular soft desorption techniques, like MALDI or electrospray ionization, which are limited, without additives, to the detection of acidic and basic compounds that can be ionized by proton transfer [54, 55]. However, analytes without basic or acidic groups can also be detected with MALDI or SALDI either by cationization or anionization, through the addition of metal salts or sulfuric acid, respectively [56, 57]. Laser ablation has also been applied for the deposition of samples on a tailored plasmonic substrate in surface-enhanced Raman microspectroscopy [58, 59].

According to this philosophy, laser-based spectrochemical analysis techniques can be classified into procedures applying (i) laser ablation purely as a sampling method, (ii) the laser-induced plasma for spectroscopic analysis, (iii) laser desorption ionization to simultaneously sample and ionize the analyte, and (iv) indirect methods. Hybrid forms are, of course, possible as well. In a nutshell, these techniques operate on the basis of laser ablation, laser desorption and the associated gaseous plasma formation, which therefore form the central processes considered in this perspective article. A deeper fundamental insight into the underlying physics of these three phenomena will open the door to further optimization and the development of new techniques. Before putting the looking glass over the fundamentals, the next section first discusses how adjusting the laser properties leads to different interaction regimes. Distinguishing these regimes will namely allow us to structure the discussion on the fundamentals even further.

## 2.2 Laser parameters affecting ablation, breakdown and desorption – the authoritarian laser regimes

Classically, the interaction of a laser with matter is described with the Beer-Lambert law, which states that the transmittance of monochromatic light through a material sample decreases exponentially with the optical path length and does not depend on the incident intensity. This corresponds to a linear light absorption process, as commonly assumed for nanosecond laser pulses [1]. Such approximation becomes invalid, however, in a high fluence regime at sufficiently long wavelengths, where the formed ablation plume effectively shields the sample from the laser [60-63]. More precisely, the laser energy is then readily absorbed by the free electrons in the plume, enabling their fast heating and the subsequent ionization of the present neutral species. This process multiplies the number of free electrons and ions as long as the ionization rate exceeds their recombination rate. Such laser-plasma interaction is no longer characterized by classical light absorption, as various non-linear effects emerge, such as direct impact and field-induced ionization and dissociation reactions and inverse Bremsstrahlung [1, 63-65]. In contrast, the plume can remain transparent to the laser light at low fluences, as any free electrons recombine with ions before they can get accelerated up to the ionization energy. Yet, the absence of a plasma in front of the sample is not a sufficient requirement for the Beer-Lambert law. Strong deviations have also been found for femtosecond pulses due to their

high peak fluence [1], where non-linear effects occur in the sample itself, including strong field ionization, inverse Bremsstrahlung and perhaps direct impact ionization.

In addition to the optical path length, the heat diffusion depth determines the ablated volume. Whereas heat diffusion is sometimes claimed to be a subordinate factor for femtosecond pulses [1], it dominates at longer time scales. The laser fluence threshold for laser ablation is namely in good approximation directly proportional to the heat diffusion depth for pico- and nanosecond pulses, with both quantities directly proportional to the square root of the pulse length [1, 66]. A strong deviation from this relationship can occur for dielectric materials already at pulse durations below 10 ps, leading to a lower threshold fluence [66, 67]. Different ablation regimes have been observed for femto- and picosecond pulses on metals as a function of fluence [68, 69], indicating a changeover between different processes with a yet unclear origin (see e.g. Figure 2). Even so, the optical penetration depth is thought to dominate in the low fluence regime, whereas thermal heat diffusion of the hot electrons should become more important in the high fluence regime [70, 71].

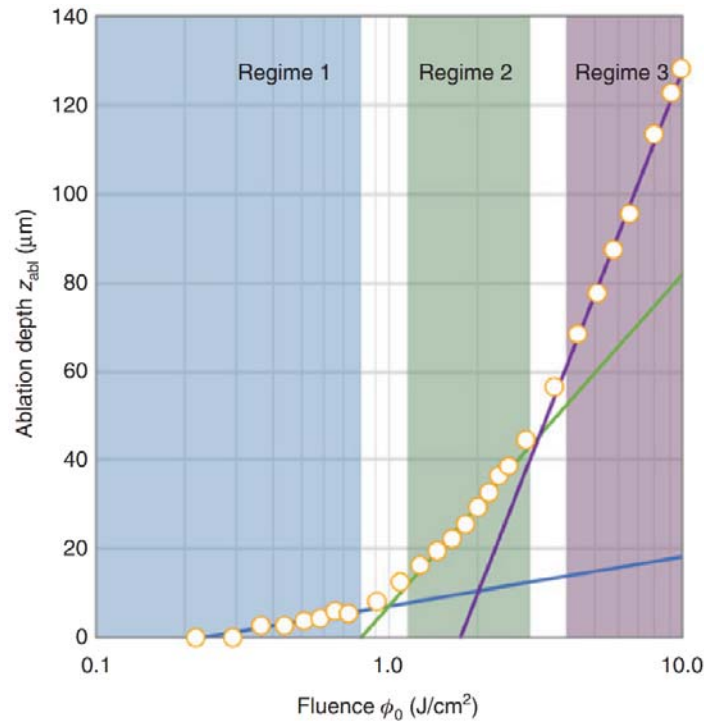


Figure 2. Three ablation regimes as a function of the laser peak fluence for copper, based on the experimental data from [72-74]. Each regime is described by an individual threshold fluence and implies distinct underlying mechanisms, which yet remain poorly understood. Reprinted from [68].

Next to the laser pulse duration and fluence, the wavelength is another crucial parameter affecting the overall ablation process, especially for nanosecond pulse durations [1, 61, 75]. Russo's group, for instance, found a lower threshold irradiance for laser ablation of silicon at a shorter wavelength, which they explained with a smaller optical penetration depth in the material and a weaker laser absorption and thus heating in the ablated laser plume [63]. In their experiments with NIST glasses and calcite samples, a shorter wavelength of incident nanosecond pulses also led to a higher reproducibility of the ablation rate [76] and a reduced fractionation [77]. Obviously, the effect of the wavelength is generally closely correlated to material properties, such as the conductivity and dielectric function,

since all of them combined determine the optical penetration depth [78]. For femtosecond pulses, however, the effect of the wavelength is much more controversial, as it is often assumed to have little influence on laser ablation, but has been observed to affect both the threshold and efficiency [1, 79, 80].

As already mentioned in Section 2.1, laser desorption/ionization is also sensitive to these laser parameters. Femtosecond pulses desorb more intact molecules as compared to nanosecond pulses, possibly due to suppression of thermal effects [81]. For the same reason, nanosecond pulses longer than 25 ns are generally not recommended [82]. Analogously, a relatively low laser fluence is preferred to prevent fragmentation of molecular analytes and promote soft desorption [82, 83], in contrast to the higher intensities applied for harder laser ablation. Moreover, shorter pulses reduce the fluence threshold for desorption [84]. In the relevant intensity range for laser desorption, however, the optimum ion yield and thus sensitivity has been observed at higher fluence values [82, 85-87]. In MALDI, the best performance is usually achieved when the wavelength approximates the absorption maximum of the matrix, when the latter is organic [88]. Besides that, infrared lasers generally produce less analyte fragmentation than their ultraviolet counterparts, making them useful for applications that require a softer ionization [84]. An extensive discussion on the effect of the fluence, pulse duration and wavelength in infrared MALDI is given in an earlier review by Dreisewerd et al. [84].

Inorganic matrices and surfaces as frequently classified under the SALDI conglomerate, on the other hand, enable application over a broad wavelength range, yet still with the highest effectivity around an absorption maximum [81, 89-91]. The underlying mechanism is unknown, but may be related to the large surface area in these materials [90]. One complicating factor is the wide variety of substrate types used in SALDI, both in composing substance and nanostructure. The mechanisms of laser absorption have been discussed in various studies for each type separately. For metallic nanoparticles, the optical absorption is attributed to the collective oscillation of conduction band electrons in response to the laser field [92-95]. It is referred to as a surface plasmon, due to the transient net charges on the particle surface during the oscillation. The surface plasmon absorption band depends on the size and strongly on the shape of the nanostructures (see Figure 3) [92, 94-96]. Irregular nanostructures, such as nanocubes and nanoprisms, typically result in wider peaks over a broad wavelength range [93, 95, 96].

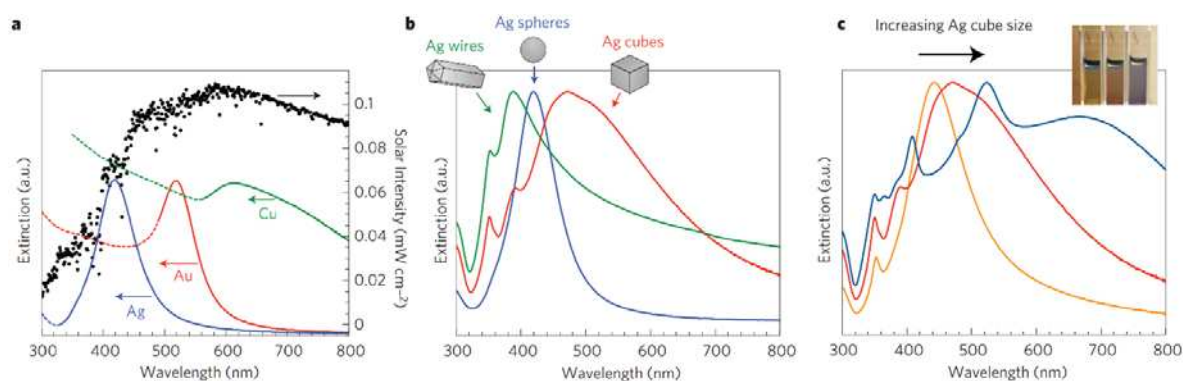


Figure 3. Comparison of normalized extinction spectra of various metallic nanoparticles. (a) Spherical Ag, Au and Cu particles, with diameters of  $38 \pm 12$  nm,  $25 \pm 5$  nm and  $133 \pm 23$  nm, respectively. Dashed portions of the curves indicate interband transitions, i.e. surface plasmon resonance is absent in these regions. The black curve represents the intensity of solar radiation. (b) Ag wires, cubes and

spheres. The wire-shaped particles have a diameter of  $90 \pm 12$  nm and an aspect ratio beyond 30. The cubic particles have a  $79 \pm 12$  nm edge length and the spherical particles a  $38 \pm 12$  nm diameter. (c) Ag nanocubes as a function of size. The orange, red and blue spectra correspond to  $56 \pm 8$  nm,  $79 \pm 13$  nm and  $129 \pm 7$  nm edge lengths, respectively. The inset displays a photograph of the nanocube samples in ethanol. Reprinted by permission from Springer Nature: Nature Materials [96], Copyright (2011).

For heavily doped semiconductor nanostructures, the optical absorption is based on the similar principle of conduction band electron oscillations, with additional absorption due to the excitation of optical phonons, interband transitions and the dielectric background of polarization generated by the tails of all the high-frequency excitations in the material [97]. This makes them particularly appealing for the entire infrared spectral window, in which their plasma frequency can be tuned with the doping density, dopant type, such as vacancy or dopant atom, and the host matrix [97, 98]. For instance, the below-bandgap infrared absorption of laser-structured silicon in SF<sub>6</sub> atmosphere was found to depend on the incorporated sulfur content [99]. This dependency was attributed to the formation of a band of sulfur impurity states overlapping with the silicon band edge. Semiconductor nanocrystals can also exhibit facet-dependent optical properties [100].

Since graphene is a semimetal, also its optical properties can be understood starting from the principle of conduction band oscillations in metals. Yet, the plasmons influence the optical properties mainly in the far-IR, in addition to free carrier absorption by intraband transitions [101-103]. In contrast, the wavelength range from near-IR to UV is dominated by interband transitions [101-103]. The optical absorption of carbon-based nanoparticles is often ascribed to electronic transitions. Carbon nanotube-based substrates, for example, exhibit wideband absorption from visible wavelengths around 635 nm up to about 3000 nm, because of the different electronic transitions in the nanotubes [104]. Carbon dots display strong absorption in the UV region and a long tail extending over the visible and into the NIR region, originating from the core and shell of the particles, respectively [105, 106]. Regarding the core contribution, the intense bands below 300 nm result from a  $\pi \rightarrow \pi^*$  transition in the aromatic C=C bonds, whereas the start of the tail from 300 to 400 nm has been assigned to a  $n \rightarrow \pi^*$  transition in C=O bonds. The spectrum at larger wavelengths is produced by surface state transitions with lone electron pairs [106]. Despite the rapidly growing knowledge on all these types of substrates, many aspects of their optical properties remain to be discovered or scrutinized. For more details on these aspects, we recommend the many review papers cited above.

In summary, different ablation, breakdown and desorption regimes have been observed as a function of the laser features, where the laser fluence, pulse duration and wavelength generally play the main roles. The regimes at a higher fluence and longer pulse duration often possess a more thermal character, allowing a thermodynamic or a combined thermodynamic and hydrodynamic picture as a decent approximation [1, 107, 108]. At lower values, the underlying processes are less understood, most likely because non-linear, resonant, collective and quantum effects become more prevalent in a complex interplay. The influence of the wavelength is only fundamentally clear in consideration of the laser-plasma plume interaction for long pulse durations, but leaves many question marks behind on the processes working in the condensed phase. Although a tremendous amount of effort has been put in basic research on these effects, an accurate and structured description of the underlying physical principles is still lacking and urgently required. In Section 3, we therefore propose an overarching

framework that transparently depicts the possible excitation and relaxation mechanisms in laser-matter interaction.

### 3. Laser-matter interaction according to the multi-plasma model

#### 3.1 The laser-initiated excitation mechanisms – so excited that you just can't hide it

In general, laser-matter interaction in spectrochemical analysis methods can roughly be subdivided into three zones: the gaseous phase, the condensed phase and the interface between them. This distinction does not have to be exclusive, since the laser will also interact in various regimes with nano- or micro-sized bubbles, droplets, particles and surface structures. In any case, considering these three zones separately can contribute to a more systematic discussion. Starting with the gaseous phase, we distinguish two effects: the plasma sheath, which makes up the topic of Section 4.2, and the laser interaction with the extracted plume. The latter only becomes relevant for long pulse durations, such as in nanosecond laser ablation. Since the extracted plume consists of electrons, ions, neutral species and charged droplets, it is best described as a complex or dusty plasma. Undoubtedly, its interaction with the laser is a complicated phenomenon, involving a combination of gaseous plasma and condensed matter excitation, as well as quantum effects related to the nanosized particles. Although we will not focus on any of these processes in specific, the mechanisms presented in the remainder of this perspective article also apply on them. The current Section and Section 3.2, for instance, deal with the laser-initiated excitation and relaxation mechanisms in the condensed phase, which are not only relevant for the initial dense sample, but also for the plume particles or droplets. The same counts for laser-induced surface phenomena, which will be further discussed in Sections 4.1 and 4.2.

Multiple excitation mechanisms have been proposed in scientific literature to explain laser interaction with a condensed phase. We first of all want to remind about the controversies in general that still persist on them until today. Secondly, research has already unequivocally pointed out the importance of the laser and sample properties, as no universal mechanism can explain every situation. Starting with the case of high enough laser intensity for ablation or breakdown, the pulse duration dictates whether or not thermal and hydrodynamic effects take place during the irradiation. For femtosecond pulses, such processes can only initiate after the irradiation has terminated. During nanosecond pulses, the balance between excitation and relaxation processes is often assumed to keep the material in an overall electrically unexcited state, where the energy of transiently excited electrons is quickly transferred to the heavy species. This permits a purely thermal description in terms of classical hydro- and thermodynamics [61]. Still, non-thermal processes may have a non-negligible contribution, especially in the initial stages of the laser interaction, keeping the transient excitation mechanisms relevant. Ultrafast pulses, however, offer the most optimal experimental conditions to study these fundamentals.

The laser wavelength further determines the nature of the excitation process. UV light is often able to cause an electronic excitation or ionization event with a single photon. In non-metallic solids and liquids, ionization corresponds in this context to the transition of a valence electron to the conduction band in the Jablonski diagram, making it quasi-free [109-112]. This is no longer possible with a single photon for longer wavelengths. In this case, excitation and ionization can still be achieved through non-linear effects caused by the high laser irradiance. More specifically, the intense stream of photons

is able as a collective whole to excite valence electrons through field-induced ionization. Due to the particle-wave duality, this mechanism can be further distinguished as a function of the intensity into multi-photon, tunnel and over-the-barrier excitation (see Figure 4) [113]. Multi-photon absorption, for instance, enables infrared lasers to elevate electrons directly over an energy interval that exceeds the energy of one of the composing light quanta. Quantum tunneling will only be possible at a higher irradiance if the tunnel ionization rate is fast enough relative to the light frequency [113]. From the moment quasi-free electrons have been generated, excitation and ionization can further eventuate through charge carrier acceleration and collisions, as well as inverse bremsstrahlung [1, 113]. This does not only count for crystalline materials, which are known to have an easily identifiable energy band scheme, but also in amorphous solids and liquids, as discussed in our earlier review [112]. Direct impact ionization, however, does not seem to be a dominant mechanism in dielectric materials, according to experimental results from a femtosecond pump-probe interferometry technique [114, 115]. Another study indicated core electron ionization via a multiphoton photochemical process for UV laser ablation of alkaline-earth metals [116].

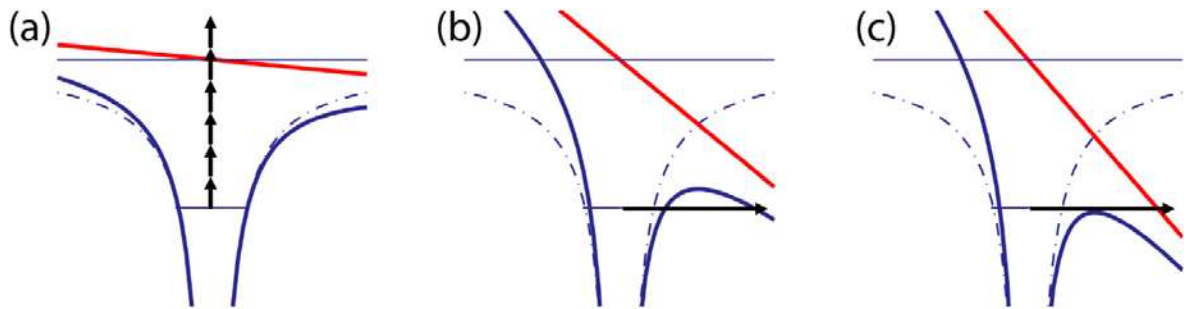


Figure 4. Schematic representation of the three strong field ionization regimes. The Coulomb potential without and with an external electric field is shown by the dashed-dotted and the solid blue lines, respectively. The red solid lines represent the corresponding external electric field from the laser beam. (a) In the multi-photon regime, multiple photons are absorbed simultaneously in order to liberate an electron. (b) The tunneling regime appears at a higher field strength, where an electron escapes by tunneling through the barrier. (c) Increasing the field even further results in the over-the-barrier regime, where the barrier is sufficiently suppressed to make the electron freely leave the atom. Reproduced from [113].

As an interesting side note, the aforementioned excitation mechanisms can serve as a source of inspiration to better understand voltage-induced breakdown of condensed materials. A classic example of this breakdown type is the plasma initiation at a high voltage pin electrode submerged in a liquid. Bubble generation prior to the plasma inception at the electrode tip can currently only be explained for voltage pulse durations of at least the order of 10  $\mu\text{s}$ , whereas plasma in pre-existing microbubbles occurs in the order of microseconds [112, 117, 118]. For sub-nanosecond pulses, however, the mechanism behind the observed rapid plasma formation at the electrode tip remains a controversial topic for now [112, 119, 120]. Therefore, we have used the parallels between voltage-

and laser-induced breakdown of liquids as a premise for our recent review article [112]. Remarkably, the fundamental insight generated in the two fields apart has largely remained isolated from one another throughout nearly a full century, explaining one of the main motivations for the above review article. For example, the possibility of quasi-free electrons and electron impact ionization in the liquid phase has been disputed for a long time by plasma physicists working on voltage-induced electrical breakdown of liquids, while the laser community welcomed these hypotheses already early on with a strikingly more open attitude [112].

Reversely, theories on voltage-induced breakdown mechanisms may also provide a more profound understanding on the laser-induced variant. An overview of such mechanisms in liquids has been given in a review by Sun et al. [121], including direct impact ionization by charge carriers, electric field dependent ionization or ionic dissociation, Auger processes, electrostriction, and breakdown in a pre-existing or generated gas bubble. More recently, we emphasized the probability of electrical discharge mechanisms involving the interface between the liquid and the submerged high-voltage electrode, such as cavities, inhomogeneous conductivity or other defects in the interfacial oxide layer [112]. Similar effects may be at play during laser ablation at a material surface or during laser-induced breakdown in the bulk phase. Nano- or microscopic cavities, for instance, can either be pre-existing at the surface or in the bulk, or get formed during the laser pulse. The former possibility especially deserves attention if the material has been subject to preceding pulses, because bubbles are plausibly formed during the rapid resolidification afterwards. Bubble formation during laser irradiation is mainly relevant for pulse durations in the nanosecond or longer time scales, analogous as in pulsed high-voltage experiments [112, 119], due to the expected slow formation time of a new bubble. Note in this regard that bubbles can act as breakdown centers because of internal gaseous plasma generation, as well as the local enhancement of the laser field.

In most of these mechanisms, the laser is assumed to interact with the material through electronic photoexcitation. In other words, any effect on the ionic cores would be indirect. Such assumption is generally allowed for UV and optical lasers, because the oscillation frequency of the electric field then surpasses the reaction rate of the heavy species due to their high inertia. This rule of thumb does not necessarily count, however, when the laser frequency approaches the vibrational levels in the material. Many intra- and intermolecular vibrations, for instance, can be excited directly with infrared light matching their energy. Such vibrational photoexcitation is thought to lie at the basis of many laser desorption ionization processes, such as in infrared MALDI [122-125]. On the other hand, MALDI with ultraviolet lasers is more likely mediated through the generation of excitons [78]. Also excitation mechanisms in SALDI may have an electronic origin, especially when inorganic nanoparticles or surface structures are used as the absorbing medium [78, 89, 91]. As expected from the low fluence associated with laser desorption ionization (see Section 3), these underlying excitation mechanisms take place at relatively low laser intensities, beyond which the aforementioned fundamental processes for laser ablation may become more dominant. Still, we believe vibrational photoexcitation and other resonant processes should not be excluded at these higher fluence regimes.

Regarding the laser interaction with matter in general and nanostructures in particular, a very interesting view has been given in 2012 by Rick Russo's and Akos Vertes' research groups in a joint perspective article [78]. More specifically, they emphasized the role of different types of quasi-particles in the laser excitation process. For bulk materials, a distinction needs to be made between metals, semiconductors and insulators. Ultraviolet lasers, for example, deposit energy in metal and

semiconductor targets at room temperature to depths of 1 to 60 nm, by exciting valence and conduction band electrons, which generates plasmons, and possibly polaritons and polarons. In contrast, semiconductors and insulators are transparent to the laser light below the multi-photon excitation threshold, if the photon energy does not resonate with optical phonons and does not reach high enough for the band gap to be crossed. In the opposite case, the laser can generate excitons and optical phonons in a direct manner. The electronic, phononic and optical features of the material depart from the bulk values when its size decreases down to the meso- or nanoscopic scale [78]. The density of states then transforms from a continuum into discrete levels, modifying the electronic and phononic spectrum as a whole.

Accordingly, we introduce the so-called multi-plasma model for electronically excited condensed matter, a conceptual framework based on non-equilibrium thermodynamics and quasi-particle physics. It considers the material as a multi-dimensional system, composed of several subsystems, each of which corresponds to one or more thermodynamic degrees of freedom. Apart from the translational degrees of freedom, all other subsystems correspond to a quasi-particle type. Figure 5 displays the variant for molecular systems. Similar to the rotational, vibrational and electronically excited degrees of freedom in a molecular gas, a molecular solid or liquid can be attributed subsystems for the librational, intramolecular vibrational modes and electronic excitations, associated with librions, vibrons and excitons as the quasi-particles, respectively. These quasi-particles may remain immobile, as if they form a solid, or can be mobilized through Förster hopping or quantum coherence between neighboring molecules, which can be seen as a phase transition into a liquid or a gas [126-128]. Note that this phase transition can transpire even if the molecules themselves remain fixed in a solid structure.

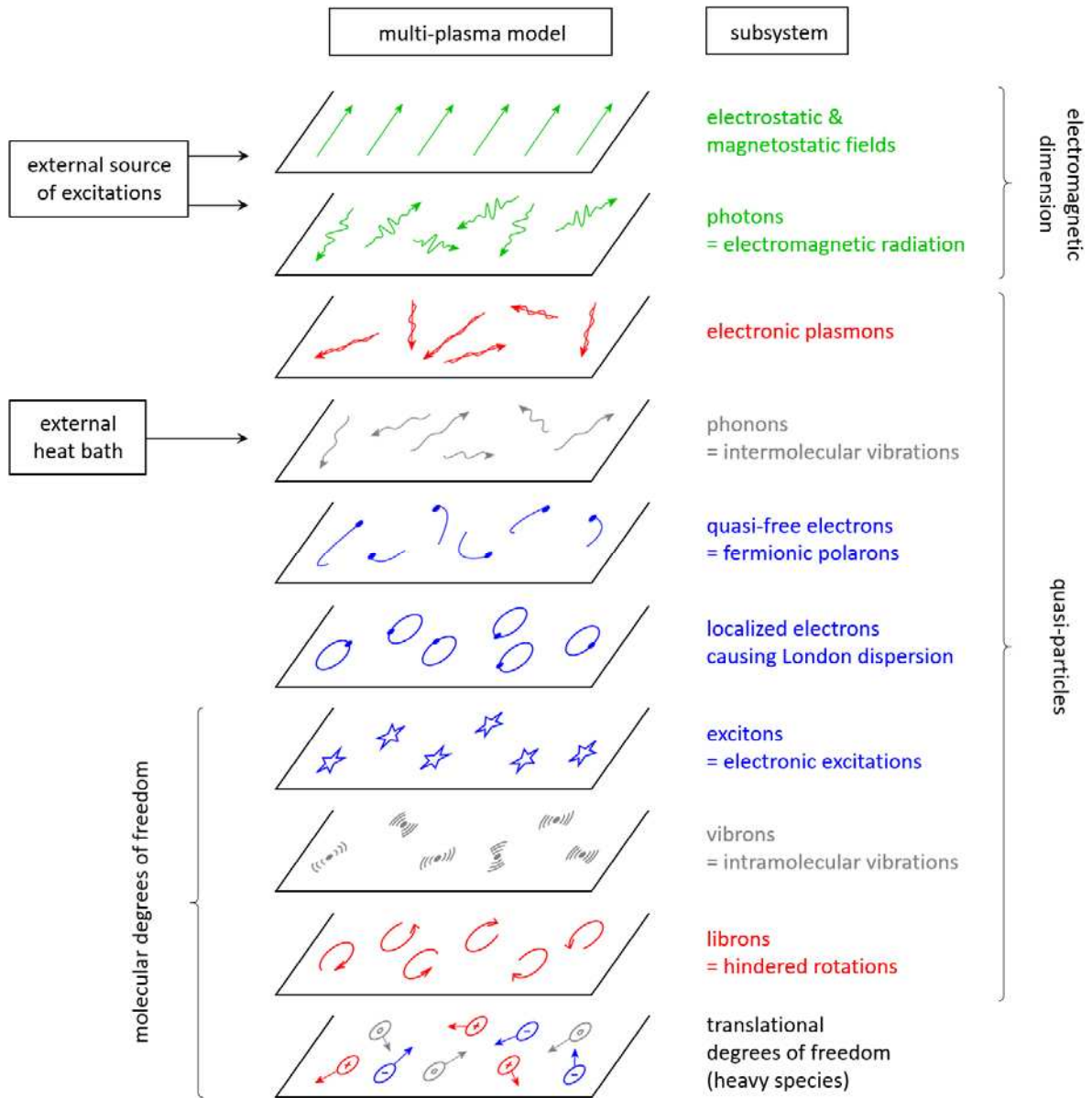


Figure 5. Schematic illustration of the multi-plasma model for laser-excited molecular systems. Note that photons are not only delivered by the incident laser, but also produced inside the system. In order to describe laser-excited non-molecular systems, the multi-plasma model is readily modified, by removing the libron and vibron subsystems.

Next to that, the phonon subsystem considers the intermolecular vibrational eigenmodes. In an amorphous system, the phonons can be further split up into propagons, diffusons and locons, based on the formulation by Fabian and Allen [129]. If the material is ionic or polar, the phonons in principle correspond to ionic or dipolar plasmons, since they then represent a collective oscillation of charge density. Electronic plasmons, on the other hand, form a separate subsystem. Obviously, the quasi-free electrons in the conduction band also make up an individual subsystem. Since these electrons carry a phonon cloud with them due to the Coulomb interactions with the neighboring atoms, dipoles or ions, they are better described as fermionic polarons. Another intriguing subsystem is associated to the quantum fluctuations of the bound electrons, which are responsible for the London dispersion

interactions. In analogy with librions, vibrons and excitons, phase transitions can also be formulated for the other quasi-particles.

The multi-plasma model serves several functions. First of all, it offers a transparent method to describe the electronically and vibrationally excited state of a material. More precisely, it maps the internal energy distribution over the different thermodynamic degrees of freedom. In this context, it is worth noting that it builds further for an important part on the phonon theory of liquid thermodynamics developed by Bolmatov, Brazhkin and Trachenko in the past decade [130]. According to this theory, the internal energy of liquid matter can be explained with a phonon formulation reminiscent to the one for solids. However, transverse phonon modes are forbidden in a solvent below a certain temperature-dependent frequency threshold, determined by the liquid relaxation time as earlier defined by Frenkel. Applying these insights, Bolmatov and his co-workers were able to calculate the heat capacity of 21 solvents solely from viscosity data, without the use of any free fitting parameters. Comparison with experimental data revealed a convincing agreement for noble, metallic, non-polar and hydrogen bonding liquids, proving the universal nature of the theory. In their later work, the authors illustrated how the phonon picture remains valid throughout all states of matter, from solid, liquid and gaseous to even supercritical conditions [131, 132]. Accordingly, the multi-plasma model adopts this universal character, making it applicable to materials undergoing any phase transition. The phonons can be understood as the carriers of potential energy in the form of vibrations, as opposed to the translational degrees of freedom, which represent the kinetic energy of the composing particles. In analogy, electronic plasmons contain the system's potential energy in the form of electron (or electron hole) oscillations, contrasted with the kinetic energy of the quasi-free electrons (or electron holes).

As a second function of the multi-plasma model, it allows a well-structured analysis of the different possible excitation mechanisms induced by a laser or any other electromagnetic stimulus. In line with the perspective of Stolee et al. [78], this implies an extension of the aforementioned excitation mechanisms with the direct photoexcitation of the quasi-particles that were not considered before, provided that they are optically active, of course. This immediately shifts the spotlight to the various types of polaritons investigated elsewhere in scientific literature [133-138]. As such, the quasi-particles mentioned in Figure 5 are far from exclusive, because new ones may need to be introduced in certain situations, for a more accurate description. The multi-plasma model thus should be seen as an adaptable and multi-functional toolbox for physicists, chemists or even biologists, working on electrically or vibrationally excited systems. Additionally, a subsystem may undergo transformations during the excitation process. In the case of a high electronic or vibrational excitation degree, both the energy structure and the populated state distribution will get modified. A clear example is a non-thermal phase transition under influence of an extreme electronic excitation [1], which softens or hardens the phonons supported by the material [139, 140]. Last, but not least, intense electric fields are expected to strongly influence the London dispersion interactions. Although the latter interactions are known to play an important role in many materials, no research has been conducted yet on this strong field effect, to the best of our knowledge.

### 3.2 Thermalization mechanisms – relaxation therapy for materials

Femtosecond laser excitation provides the right conditions to study the elementary processes in the irradiated material, due to the sufficiently short laser pulse in comparison to the duration of these processes. Figure 6 gives such comparison with thermalization mechanisms, charge carrier removal, thermal and structural effects. The ultrashort laser pulse instantly brings the material in a strong non-equilibrium characterized by hot electrons and cold ions by means of the excitation mechanisms described in Section 3.1. After the pulse has ended, the electrons transfer their energy to the ions in a sub-picosecond timeframe through electron-phonon coupling. This heats up the phonon bath before slow thermal effects can restructure the material [141-144]. In metals, the electrons and phonons will reach the same temperature this way, allowing any succeeding thermal phase transition to take place while the system resides in an internal equilibrium. In semiconductors and insulators, the generated excitons will additionally recombine through radiative or non-radiative recombination, where the latter implies an exchange with phonons [78]. As a computational study by the Rethfeld group has demonstrated for copper, the non-equilibrium in the quasi-free electron subsystem can last as long as the non-equilibrium in the phonon subsystem, bringing both subsystems in equilibrium with each other on a timescale of about 10 ps [145]. Simulations on silicon, however, revealed a non-equilibrium in the phonon subsystem for several hundreds of picoseconds [146]. Such non-equilibria may therefore influence the early stage of thermal effects. In this regard, it seems more advised to think in terms of non-thermal and thermal timescales, rather than non-thermal and thermal processes.

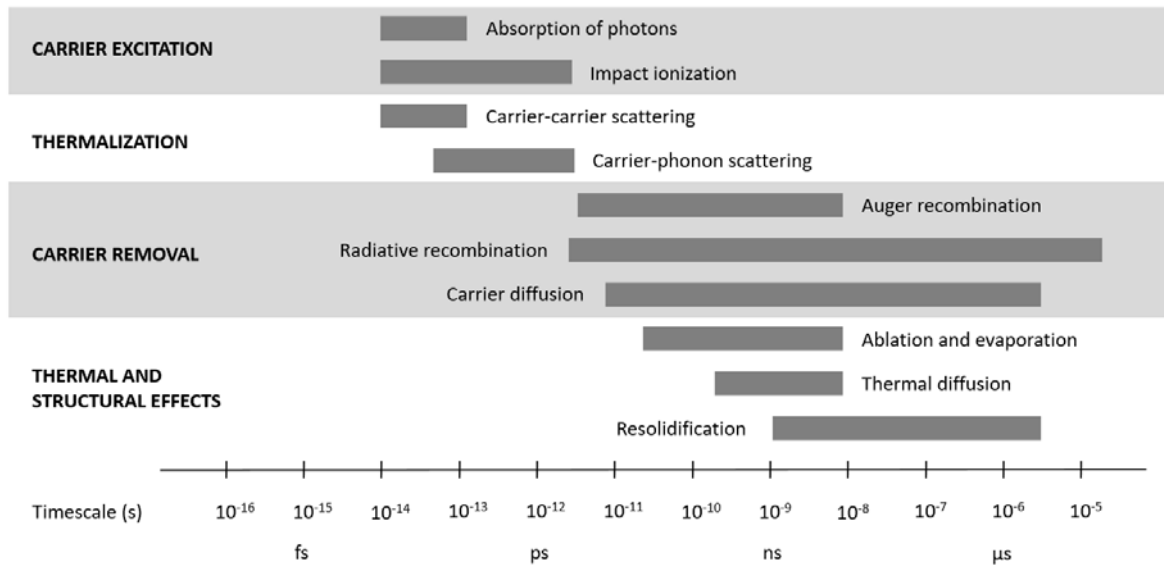


Figure 6. Fundamental processes during femtosecond laser ablation and their characteristic time scales. Adapted by permission from Springer Nature: Nature Materials [142] based on [147], Copyright (2002).

This description of the laser-induced processes in the material is based on the two-temperature model, introduced by Anisimov et al. [148, 149], which attributes two distinct temperature values to the quasi-free electrons and the lattice. Despite its simplifying assumptions, such as a neglect of other types of excited states, this two-temperature picture has found a successful application in many research studies. Molecular dynamics simulations built on the model have namely delivered numerous insightful results for metals on the laser-induced phase transitions, material restructuring and mass transfer (see e.g. [150-157]). The introduction of the multi-plasma model in Section 3.1 needs to be

understood as our proposal to extend the two-temperature model to a multi-temperature model. Every thermodynamic degree of freedom can namely be characterized with a distribution function, for which a temperature may be defined. The higher dimensionality of the multi-plasma model should lead to a higher accuracy of the simulation results and a more profound insight into the underlying processes.

Moreover, it directly reveals alternative thermalization pathways between the different subsystems. The equilibration between the quasi-free electron and plasmon subsystems, for instance, can partly determine the temporal evolution of the non-equilibrium electron distribution function [158-161]. After each ionization event, for instance, various subsequent processes involving plasmons can be expected. An example is given in Figure 7, depicting the excitation of an electron in gold and the succeeding relaxation mechanisms, with the possible emission of a plasmon [162]. From these two subsystems, different parallel thermalization channels can further be identified towards the heavy species. As a general insight from plasma physics, the coupling between mobile and bound electrons dominates over the electron-ion coupling [163]. The exciton subsystem is therefore expected to play an important role in the thermalization towards the subsystem of the heavy species. In the case of direct vibrational photoexcitation, a two- or multi-temperature model can analogously be applied. The non-equilibrium in the phonon subsystem deserves here additional attention, because it may lead to important effects, such as multiphonon up-pumping, i.e. the fusion of two or more phonons with the generation of a more energetic rotational or vibrational mode [164, 165].

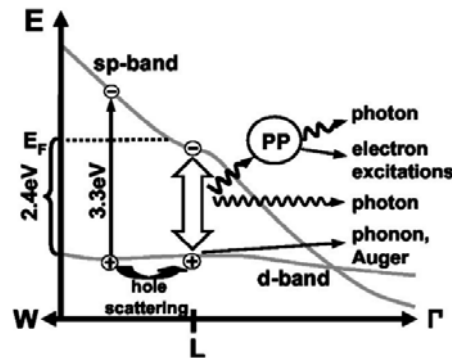


Figure 7. Energy scheme of  $d \rightarrow sp$  interband excitation and subsequent hole relaxation close to the L point of the band structure of gold. A photon with 3.3 eV energy promotes electrons from the d-band into the sp-band sufficiently above the Fermi level. The photoexcited d-band holes undergo Auger scattering and hole-phonon scattering. Direct radiative recombination of a d-band hole with an electron in the sp band below the Fermi surface or scattering to the conduction band with via the emission of a plasmon particle (PP) may occur. The plasmon subsequently decays either radiatively or nonradiatively. Reprinted figure with permission from [162]. Copyright (2004) by the American Physical Society.

The material surface needs to be considered as a separate zone with its own excitation and thermalization mechanisms, due to the presence of surface states and the formation of a net charge after electron emission. The multi-plasma model especially lends itself for the description of surface nanostructures, such as the laser-induced periodic surface structures formed during successive pulses [166-169]. That is, at a time scale comparable to the quasi-particle relaxation times and at a length scale similar to the quasi-particle mean free paths, the quasi-particles travel unimpeded through the

structure and scatter primarily at the interface. Heat and thus phonon transport, for instance, behaves in a diffusive manner in macroscopic objects over a long time, but becomes ballistic in nature when the length and time scales are narrowed down, where the mean free path of the phonons can be as large as 300 nm, but decreases with temperature [78, 170]. Regarding the relaxation of electronic excitations, the luminescence observed from the nanostructures is attributed to recombination processes from defect centers and quantum confinement [78].

#### 4. Laser sputtering mechanisms

##### 4.1 Mass transfer and phase transitions – faster than greased lightning

The excitation and thermalization processes in the laser-irradiated material result in rapid heating of the phonon bath. For femtosecond laser pulses, the rapid energy deposition causes so-called inertial stress confinement [68, 157, 171, 172], due to the buildup of strong compressive stresses and the inability of the material to expand in such short timeframe. The subsequent relaxation of these stresses generates sub-surface voids, leading to the separation of liquid surface layers and the ejection of droplets [68]. For this reason, heat conduction and hydrodynamic motion remain limited during an ultrafast laser pulse, reducing the thermal damage and heat affected zones on the target [173]. Two explosive regimes can occur, starting with photomechanical spallation at lower fluences, to phase explosion at higher ones [68, 107]. For longer or consecutive pulses, also strong recoil pressures up to 1 GPa have been reported [174], but shielding of the laser beam by the ejected plume can play a role, especially at longer wavelengths. This significantly reduces the ablation efficiency as compared to femtosecond pulses [175]. However, the ablation efficiency can still be high for nanosecond pulses at shorter wavelengths, where the inverse Bremsstrahlung in the laser-plume interaction is negligible [1].

Figure 8 shows the temporal transmission of the plumes from metal targets for a probe wavelength of 400 nm. A first transmission drop below 20% is observed around 5 ns after the ablating femtosecond laser pulse, caused by plasma shielding. Around 150 to 200 ns later, another less extreme minimum appears, which has been attributed to a particle shielding effect, where the light is assumed to be Mie-scattered by the particles emitted from the ablation process [70, 176]. In this context, it is worth noting three studies by Russo's group, one of which investigated the particle size and shape [177], and two of which focused on a delayed particle emission effect [178, 179]. Femtosecond pulses on brass were found to produce particles of around 100 nm in diameter that formed large agglomerates, while nanosecond pulses generated spherical entities ranging from several hundreds to thousands of nanometers [177]. According to the other two studies, laser pulses on silicon with a 3 ns duration first removed mass during the pulse by normal evaporation, followed after 300 to 400 ns by the ejection of micron-sized particulates due to delayed explosive boiling [178, 179]. This delay was explained with the retarded nucleation and growth of bubbles in the superheated melt. Note that such mechanism may also be valid for femtosecond pulses. The limited heating of the material surrounding the melt in the femtosecond case may even underlie the absence of a raised rim above the surface [77], in contrast to nanosecond laser ablation.

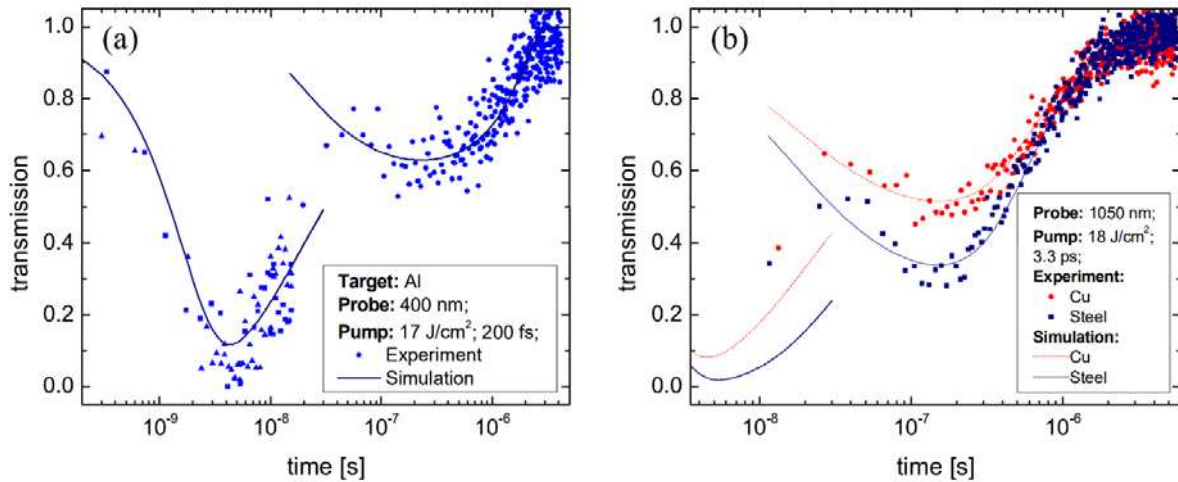


Figure 8. Transmission of probe light through the ablated plume as a function of the delay time between the pump and probe laser pulses for (a) an Al target and (b) Cu and steel targets. The probe wavelength, pump peak fluence and pulse duration are given in the inset of each graph. Reproduced from [176].

Still many questions remain on the origin of molecular species in the ablated plume, since they may be emitted by evaporation or as by-products from photomechanical spallation or phase explosion, either directly from the sample surface or from ejected nanoparticles or droplets. In the case of femtosecond pulses, the molecular fragment production has been found to be high for a wide wavelength and fluence range [62], and also depends on the position of the laser focus relative to the sample surface [180]. Nanosecond pulses, in contrast, are less suitable to retain the molecular structures, for both infrared and ultraviolet wavelengths. For infrared, this is due to the low molecule production rate at low fluences and the plasma heating by the laser-plume interaction at higher ones [62]. Nanosecond ultraviolet pulses do not present this shielding effect, but are more likely to break molecular bonds by the high photon energy and strong thermal effects.

The angular distribution at which the ablated species and particles are emitted strongly depends on the laser parameters. As shown in Figure 9, femtosecond pulses generate a significantly narrower distribution [181-183], attributed to the inertial stress confinement caused by the low optical penetration depth and greater power per unit volume [184, 185]. In nanosecond laser ablation, the ablated plume is sharpened for increasing laser spot sizes, which has been explained by Harilal et al. with ion acceleration from enhanced laser-plasma coupling [1, 186]. The exact underlying mechanism is, however, still a matter of dispute. Russo's group, for instance, additionally observed a higher phase explosion irradiance threshold at a larger beam spot size and indicated the plasma expansion dynamics as the main origin [63], which can as well explain the plume sharpening.

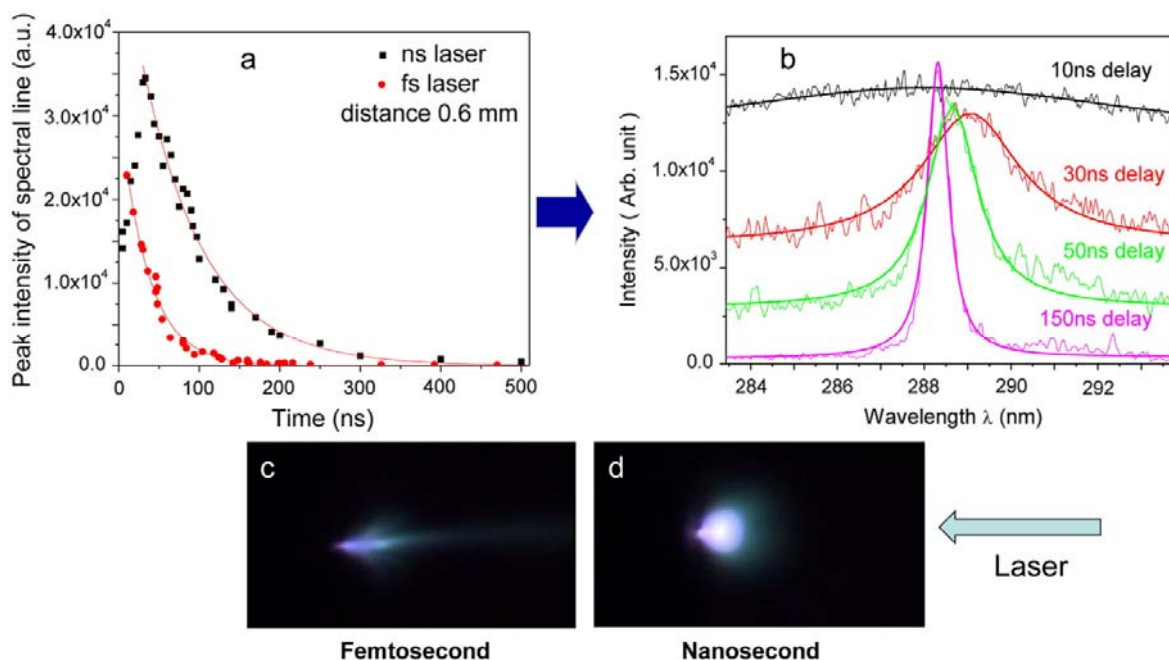


Figure 9. Some characteristics of femto- and nanosecond pulsed laser-induced plasmas, with (a) the persistence of plasma, (b) the emitted UV spectrum measured for ablation of silicon as a function of time, showing the change in background, spectral line shifting and broadening, and (c)-(d) optical photograph of the plasmas. Adapted with permission from [187]. Copyright (2013) American Chemical Society.

Laser parameters also influence the fractionation of trace elements. Once more in Russo's group, experiments were conducted to investigate the effect of pulse duration and wavelength on the emitted elemental Pb/U, Pb/Th and Pb isotopic ratios from NIST glass samples [77, 188]. For infrared light, both femtosecond and nanosecond pulses led to significant fractionation. At ultraviolet wavelength, a reduced fractionation was observed, with the best performance for femtosecond pulses. Comparison of measurements on monazites and zircon samples revealed UV femtosecond LA-ICP-MS calibration to be less matrix-match dependent and thus more versatile [188]. The authors explained the effect of the pulse duration with the higher irradiance of the femtosecond laser, which, they believed, led to negligible thermally induced fractionation [188]. For the effect of the wavelength, they mentioned the different degree in gaseous plasma formation, laser-plume interaction and generated shock waves as possible contributions [77]. We propose, however, a plausible alternative explanation, based on their delayed explosive boiling model. Fractionation may namely be due to a separation of the elements in the superheated melt before explosive boiling occurs. Perhaps, the separation rate is then influenced by the wavelength through a variation in mixing or a surface field-induced phase separation in the melt. Sections 4.2 and 4.3 throw a light on how these effects can come about.

Two even more controversial mass transfer mechanisms in laser ablation are electrostatic ablation and Coulomb explosion. Both assume the release of ions from the sample surface directly into the gas phase through strong field effects. As a first step, the laser creates a positively charged surface layer, either by means of the photoelectric effect for sufficiently short wavelengths, or by field-assisted thermionic emission. According to the electrostatic ablation mechanism, the surface ions are

subsequently pulled into the gas phase by the electric field induced by the emitted electrons [108, 189]. In contrast, a Coulomb explosion occurs as an effect of the repulsive forces between the positive ions in the surface layer [108, 189]. These mechanisms should be ultrafast, and therefore may explain the emission of ions in the early stage of the femtosecond pulsed ablation (see Figure 10). As the main criticism, nonetheless, the surface charge may be rapidly eliminated by charge compensation processes, such as the redistribution of conduction electrons from the bulk, making these mechanisms strongly debated [1].

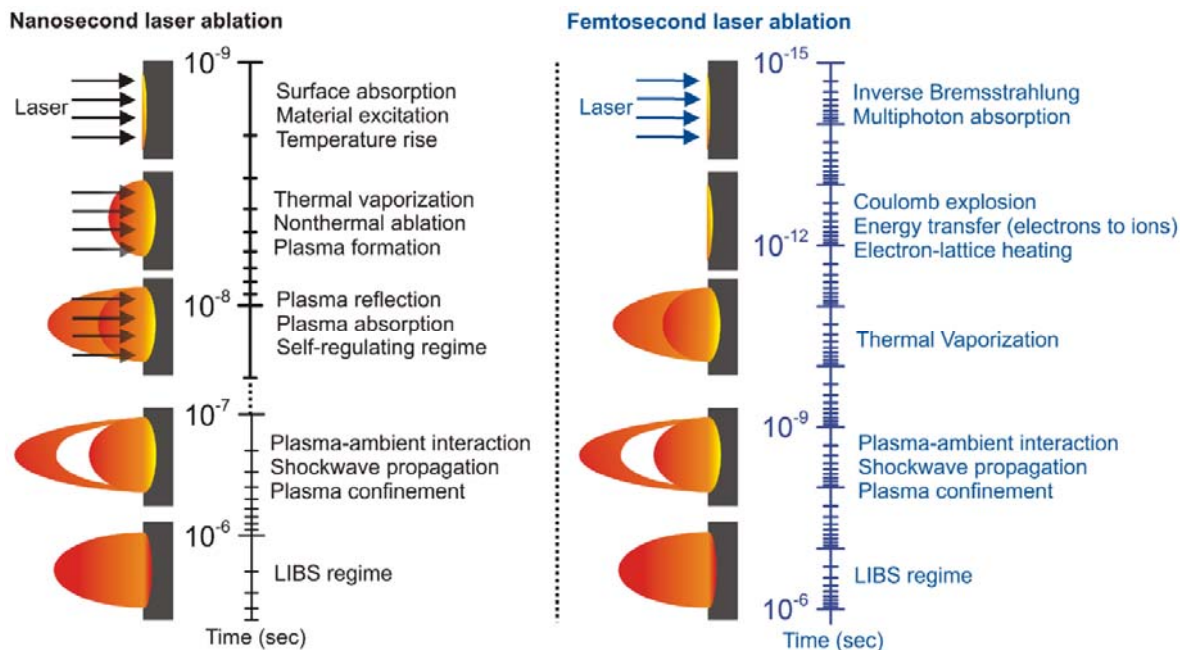


Figure 10. Timescales of various processes taking place during and after the laser pulse in (left) nanosecond and (right) femtosecond laser ablation. Reproduced from [1].

Up to now, there is also still no agreement on the principle underlying resonant laser ablation. For metal targets irradiated with a tuned UV laser, the most accepted theory assumes a fraction of the laser energy to be deposited in the sample, producing a low density vapor, while another part interacts with the vapor plume through a resonant ionization process [39, 190]. Mid-infrared excitation of polymeric targets is often considered to be a photothermal process, where the laser can be approximated as a heat source and the main ablation mechanism consists of a phase change followed by vaporization of the material [42, 191]. Molecular desorption with visible or ultraviolet wavelengths, on the other hand, is more likely mediated through electronic excitations, which can result in various desorption mechanisms in analogy with MALDI and SALDI (see e.g. the reviews by Dreisewerd et al. [83] and Stolee et al. [78] for a more detailed discussion of such processes). In the case of SALDI, however, more recent studies have convincingly indicated the contribution of thermal desorption and phase transition of the supporting inorganic material to be major mechanisms driving the extraction [192-197]. The underlying thermal desorption allows to increase the emitted ion fraction, by selecting substrates that display a stronger heat confinement [192, 196] and a weaker binding interaction with the analyte molecules [193, 195, 197]. In addition, the phase-transition-driven desorption can be straightforwardly enhanced by lowering the melting temperature [193-195] or the phase explosion threshold [197] of the inorganic nanostructures.

As described in Section 3.2, quasi-free electrons and electronic excitations may first transfer their energy to the phonon bath in a few picoseconds. The vibrational energy can subsequently lead to desorption processes, e.g. through multiphonon up-pumping at the surface. As a second possibility, an electron gas or electronic excitations in the substrate can transfer their energy directly to a neighboring adsorbate. Thirdly, an electronic excitation in the adsorbate itself may generate a repulsive state, followed by a desorption event. Obviously, this requires an excitation energy exceeding the surface bond energy. The latter mechanism is also known as desorption induced by electronic transition (DIET). Combined processes have also been suggested, such as simultaneous phonon and exciton generation, driving a phase transition in the matrix and the ionization process, respectively [78]. The cluster ionization mechanism proposed by Karas et al., for instance, considers pre-charged ions in the matrix to be precursors of ions emitted into the gas phase [198]. A unique mechanism for laser desorption in e.g. MALDI or SALDI therefore does not exist.

#### 4.2 Laser-induced ionization and the plasma sheath – where the debate gets truly charged

As discussed in Section 2.1, several laser-based spectrochemical analysis methods, including LIBS, MALDI and SALDI, rely on the plasma properties of the extracted plume. This underlines the importance of the ionization degree in the plume, which partly determines the optical emission spectrum and intensity for LIBS or the measurement sensitivity for mass spectroscopy techniques without an intermediate ionization method, such as MALDI-MS and SALDI-MS. Despite the countless investigations on this aspect, the fundamental origin of the plume ions is still poorly understood [9]. A priori, the following diverse sources can be distinguished:

- 1) At sufficiently high fluence, the laser beam is able to directly ionize gas phase species by strong field ionization, single- or multi-photon absorption.
- 2) Electrons emitted from the sample surface due to the photoelectric effect, field-induced and thermionic emission enable direct impact ionization in the surrounding gas [199].
- 3) Individual ions may be directly transferred from the condensed phase into the gas phase through ion desorption or more violent processes like electrostatic ablation and Coulomb explosion.
- 4) The laser-induced dense plasma can expand with a preservation of ionic species [47].
- 5) When charged droplets or nanoparticles are ejected from the sample, they may automatically reduce in size by evaporation or division processes such as Coulomb fission, much like in electrospray ionization. Alternatively, the particles can transfer charge to colliding neutral gas species.
- 6) Charge transfer processes may also occur between hot neutral species, as an effect of their kinetic energy or by chemical processes.
- 7) Any formed gas phase plasma can further interact with the laser beam, especially for long wavelengths and pulse durations.

Each of these mechanisms has indeed been proposed in scientific literature to explain experimental observations. Obviously, their relative dominance strongly depends on laser parameters like fluence, wavelength and pulse durations, as well as material properties, such as the work function, ionization energy, molecular structure, surface structure and so on. In general, however, the ionization efficiency of laser-sample interaction is low, no matter whether the technique is based on laser ablation, LIBS,

laser desorption or LIAD [9]. The yield of analyte ions is namely far lower than the one of neutrals, even if an organic matrix is used to assist ionization [200]. Neutral species therefore strongly contribute to the optical emission spectrum. Still, the spectrum in laser ablation generally contains continuum emission that has been attributed to free-free and free-bound transitions, next to spectral broadening of the emission lines caused by the Stark and Doppler effect [1, 2]. After the pulse has ended, plasma expansion and cooling result in relatively sharp spectral line emission instead (see Figure 9(b)) [1, 2, 201]. Note, in this regard, that one element in the laser plume can interfere with the emission from another element by inhibiting the ionization of the latter, which partly explains the influence of the matrix, next to fractionation [2]. In comparison to nanosecond lasers, ablation by femtosecond pulses produces a lower temperature plasma, less continuum emission and a relatively stronger emission from neutral species, with molecules in particular, for a shorter time (see Figure 9(a)) [1].

In picosecond ablation of metal targets in air atmosphere, Russo's group observed an early-stage plasma before the release of a material vapor plume, which was explained as a longitudinal expansion of an ionization front triggered by the air breakdown by electron emission from the target [199]. Such phenomenon has been further supported by an investigation of Bulgakova et al. [202], focused on the charging effects, Coulomb explosion and plasma etching of the irradiated surface. This implies a plasma sheath formation on very short time scales. We want to emphasize the importance of such sheath, as it corresponds with a locally strong electric field at the material surface. This field will influence many other processes at the surface, including excitation and thermalization mechanisms, charging, mass transfer and ionization. The lifetime of this sheath is an especially crucial factor, as it imposes an outward force on the surface, which may contribute to surface deformations and instabilities at a later stage. The study of this laser-induced plasma sheath is on its turn complicated by the presence of surface roughness, protrusions and nanodroplets. This immediately leads to another research question that has not received much attention yet: how does the plasma sheath around ejected droplets and nanoparticles contribute to their evolution and the plume process in general?

Another interesting question has been put forward by Cai et al. in their review [47], namely how electronic levels and excitations behave in a dense plume, like the one produced in laser ablation. The authors developed a model for laser-excited atomic fluorescence of such plume, but it can as well be considered for the expansion of a dense plasma. According to the model, the wavefunctions of the composing neighboring atoms would strongly interact as long as their density remains sufficiently near solid or liquid density. In laser ablated plumes with a typical density of  $10^{20} \text{ cm}^{-3}$ , for instance, the inter-particle distance is about 2 nm. Under these conditions, excited states can form bands, delocalizing the electrons [47]. Therefore, one can no longer reason in terms of gas phase values to model such dense plumes. Once excited, these excited states would relax both non-radiatively and radiatively, contributing to continuum emission. After expansion of the plume to much lower densities, the radiating atoms would instead emit sharp spectral lines [47].

Closely related is the question about the origin of gaseous ions in laser desorption ionization. This topic has inspired many competing theories. The cluster ionization mechanism by Karas et al. for MALDI, which assumes pre-charged ions in the matrix to be precursors of the emitted ions [198], is one example. Knochenmuss et al. present in their review [203] several in-plume mechanisms for the formation of analyte ions, including proton transfer, cation transfer, electron transfer and electron capture, as well as the role played by clusters. Another interesting review in this regard is the one by

Lu et al. [55], which reveals the often made mistake not to distinguish between the ion-to-neutral ratio for the analyte and the matrix molecules in MALDI, as these can diverge strongly. The latter authors additionally described and applied a thermal proton transfer model to explain the produced ion-to-neutral ratios and total ion intensity. Similar ionization mechanisms have been proposed for SALDI, such as the thermal-driven ionization mechanism, proton transfer, cation transfer, photoelectron transfer, nanophotonics-based ionization, and hot carrier-enhanced ionization, as more thoroughly discussed in a review by He et al. [204]. The wide variety in energy transfer media makes a case-to-case study unavoidable for MALDI and SALDI.

#### 4.3 Anisotropy and magnetic effects – asking for directions

Last, but not least, we want to put the attention on two effects that are often neglected, yet might have a substantial contribution to the overall laser ablation or desorption process. First of all, there are several reasons to expect anisotropic processes during the laser-sample interaction. The presence of the surface implies anisotropic conditions, as already illustrated in Section 4.1 with the role of surface states and in Section 4.2 with the emergence of a plasma sheath. Yet, anisotropy may also occur closer to the sample bulk, due to the polarization and incident angle of the laser. These laser parameters may cause a direction dependency in the excitation and relaxation mechanisms. Linearly polarized laser light could, for instance, lead to an anisotropic non-thermal phase transition. Such directional effects have, to our knowledge, not been confirmed or refuted yet with experiments or simulations.

Moreover, strong laser-induced currents in the condensed material allow the generation of long-lived magnetic fields. Self-generated magnetic fields have been detected for laser-induced plasmas in gaseous and solid targets with amplitudes up to the order of  $10^4$  T [205-207], explained with various mechanisms [208-211]. Clearly, such strong local fields can deform the plasma sheath, affect the excitation and relaxation mechanisms and also cause an overall anisotropy in the laser-material interaction. Therefore, a detailed investigation of these influences is desirable.

## 5. Conclusion

In a nutshell, this perspective article gives a short overview of the fundamental principles behind spectrochemical analysis technology, and highlights some of the most pressing questions for future research. The techniques have been classified into four groups according to the function of the laser, namely (i) laser ablation purely as a sampling method, (ii) the laser-induced plasma for spectroscopic analysis, (iii) laser desorption ionization to simultaneously sample and ionize the analyte, and (iv) indirect methods. Correspondingly, these techniques operate on the basis of laser ablation, laser desorption and the associated gaseous plasma formation, which have been chosen as the central processes for this perspective article. For a structured discussion on their fundamentals, these processes need to be further subdivided into distinct regimes. This is in general possible as a function of the laser fluence, pulse duration and wavelength.

These laser parameters strongly determine the excitation mechanisms in the dense sample. The wavelength decides whether excitation or ionization occurs through the absorption of a single photon

or requires the collective effect of the laser beam light quanta through strong field ionization. The latter mechanism can be split up as a function of the fluence rate into multi-photon, tunnel and over-the-barrier excitation. The pulse duration dictates the timing of these excitation mechanisms relative to the induced thermal effects. Impact ionization and inverse bremsstrahlung are two other mechanisms often considered in literature, which allow further excitation of the system once quasi-free charge carriers have been generated. We, however, strongly recommend not to consider this list of popular excitation mechanisms to be exclusive. First of all, surface features and defects, such as gas cavities, in the irradiated zone may play an important role in the laser-induced breakdown process. Secondly, light is also able to induce other collective excitations in a direct manner, such as plasmons and several types of vibrational modes. Following this line of thought, we have briefly introduced the so-called multi-plasma model, which transparently presents the multiple thermodynamic dimensions in the condensed system by means of different quasi-particle types. This model also gives a clear picture of the possible thermalization channels between the quasi-particle subsystems, facilitating a discussion beyond electron-phonon coupling alone. Indeed, the heated quasi-free electrons may transfer their energy to several subsystems simultaneously, a possibility that is often overlooked in scientific literature. Moreover, we believe that the multi-plasma model can serve as a building platform for more advanced computational models, which has already been precluded with the computational application of the two-temperature model.

Laser-induced mass transfer and ionization mechanisms can roughly be distinguished into a thermal group, including normal evaporation, photomechanical spallation and phase explosion, and a non-thermal group, including desorption induced by electronic transition, electrostatic ablation, Coulomb explosion and various proposed LDI mechanisms for MALDI and SALDI. In this regard, we have emphasized the delayed explosive boiling model developed by Rick Russo's group, as well as the possible role of the laser-induced plasma sheath. Additionally, quantum effects should be considered in the transition from a condensed to a gaseous phase, because the wavefunctions between the ground state and excited species are expected to keep interacting up to an interparticle distance of about one to a few nanometers in the intermediate state, depending on the excitation degree. Finally, anisotropic and magnetic effects have largely been disregarded up to now, although there are indications that they may have a significant contribution to many of the aforementioned mechanisms. By bringing this manifold of fundamental questions to the foreground, we hope to motivate more basic research on laser-matter interaction, as a continuation of the lifework of Rick Russo, to whom we devote this perspective article.

## REFERENCES

1. Harilal, S., et al., *Optical spectroscopy of laser-produced plasmas for standoff isotopic analysis*. Applied Physics Reviews, 2018. **5**(2): p. 021301.
2. Harmon, R.S., R.E. Russo, and R.R. Hark, *Applications of laser-induced breakdown spectroscopy for geochemical and environmental analysis: A comprehensive review*. Spectrochimica Acta Part B: Atomic Spectroscopy, 2013. **87**: p. 11-26.
3. Singh, V.K., et al., *Elemental Mapping of Lithium Diffusion in Doped Plant Leaves Using Laser-Induced Breakdown Spectroscopy (LIBS)*. Applied Spectroscopy, 2019. **73**(4): p. 387-394.
4. Choi, S.H., et al., *Heavy metal determination by inductively coupled plasma-mass spectrometry (ICP-MS) and direct mercury analysis (DMA) and arsenic mapping by*

- femtosecond (fs)–laser ablation (LA) ICP-MS in cereals*. Analytical Letters, 2019. **52**(3): p. 496-510.
5. Guinan, T., et al., *Surface-assisted laser desorption ionization mass spectrometry techniques for application in forensics*. Mass spectrometry reviews, 2015. **34**(6): p. 627-640.
  6. Orellana, F.A., et al., *Applications of laser-ablation-inductively-coupled plasma-mass spectrometry in chemical analysis of forensic evidence*. TrAC Trends in Analytical Chemistry, 2013. **42**: p. 1-34.
  7. Bonta, M., et al., *Elemental mapping of biological samples by the combined use of LIBS and LA-ICP-MS*. Journal of Analytical Atomic Spectrometry, 2016. **31**(1): p. 252-258.
  8. Wang, H., et al., *Advances in ICP-MS-based techniques for trace elements and their species analysis in cells*. Journal of Analytical Atomic Spectrometry, 2017. **32**(9): p. 1650-1659.
  9. Cheng, S.-C., et al., *Laser-based ambient mass spectrometry*. Analytical Methods, 2017. **9**(34): p. 4924-4935.
  10. Herdering, C., et al., *Laser ablation based bioimaging with simultaneous elemental and molecular mass spectrometry: towards spatially resolved speciation analysis*. Rapid Communications in Mass Spectrometry, 2013. **27**(23): p. 2588-2594.
  11. Herdering, C., et al., *Ambient molecular imaging by laser ablation atmospheric pressure chemical ionization mass spectrometry*. Rapid Communications in Mass Spectrometry, 2013. **27**(23): p. 2595-2600.
  12. Shelley, J.T., S.J. Ray, and G.M. Hieftje, *Laser ablation coupled to a flowing atmospheric pressure afterglow for ambient mass spectral imaging*. Analytical chemistry, 2008. **80**(21): p. 8308-8313.
  13. Stopka, S.A., et al., *Ambient metabolic profiling and imaging of biological samples with ultrahigh molecular resolution using laser ablation electrospray ionization 21 tesla FTICR mass spectrometry*. Analytical chemistry, 2019. **91**(8): p. 5028-5035.
  14. Nemes, P. and A. Vertes, *Laser ablation electrospray ionization for atmospheric pressure, in vivo, and imaging mass spectrometry*. Analytical chemistry, 2007. **79**(21): p. 8098-8106.
  15. Compton, L.R., et al., *Remote laser ablation electrospray ionization mass spectrometry for non-proximate analysis of biological tissues*. Rapid Communications in Mass Spectrometry, 2015. **29**(1): p. 67-73.
  16. Zou, J., et al., *Ambient mass spectrometry imaging with picosecond infrared laser ablation electrospray ionization (PIR-LAESI)*. Analytical chemistry, 2015. **87**(24): p. 12071-12079.
  17. Zhang, L.X. and R.K. Marcus, *Mass spectra of diverse organic species utilizing the liquid sampling-atmospheric pressure glow discharge (LS-APGD) microplasma ionization source*. Journal of Analytical Atomic Spectrometry, 2016. **31**(1): p. 145-151.
  18. Paing, H.W., et al., *Coupling of Laser Ablation and the Liquid Sampling-Atmospheric Pressure Glow Discharge Plasma for Simultaneous, Comprehensive Mapping: Elemental, Molecular, and Spatial Analysis*. Analytical Chemistry, 2020.
  19. Cahill, J.F., V. Kertesz, and G.J. Van Berkel, *Characterization and application of a hybrid optical microscopy/laser ablation liquid vortex capture/electrospray ionization system for mass spectrometry imaging with sub-micrometer spatial resolution*. Analytical chemistry, 2015. **87**(21): p. 11113-11121.
  20. Ovchinnikova, O.S., V. Kertesz, and G.J. Van Berkel, *Combining laser ablation/liquid phase collection surface sampling and high-performance liquid chromatography– electrospray ionization-mass spectrometry*. Analytical chemistry, 2011. **83**(6): p. 1874-1878.
  21. Wang, X., et al., *Sub-microanalysis of solid samples with near-field enhanced atomic emission spectroscopy*. Spectrochimica Acta Part B: Atomic Spectroscopy, 2018. **141**: p. 1-6.
  22. Ellis, S.R., et al., *Surface analysis of lipids by mass spectrometry: more than just imaging*. Progress in lipid research, 2013. **52**(4): p. 329-353.

23. Nyadong, L., et al., *Atmospheric pressure laser-induced acoustic desorption chemical ionization mass spectrometry for analysis of saturated hydrocarbons*. Analytical chemistry, 2012. **84**(16): p. 7131-7137.
24. Babushok, V., et al., *Double pulse laser ablation and plasma: Laser induced breakdown spectroscopy signal enhancement*. Spectrochimica Acta Part B: Atomic Spectroscopy, 2006. **61**(9): p. 999-1014.
25. Li, K., et al., *Laser ablation assisted spark induced breakdown spectroscopy on soil samples*. Journal of Analytical Atomic Spectrometry, 2010. **25**(9): p. 1475-1481.
26. Liang, Z., et al., *Tip-enhanced ablation and ionization mass spectrometry for nanoscale chemical analysis*. Science advances, 2017. **3**(12): p. eaaq1059.
27. Jabbour, C., et al., *Development of a tip enhanced near-field laser ablation system for the sub-micrometric analysis of solid samples*. Journal of Analytical Atomic Spectrometry, 2016. **31**(7): p. 1534-1541.
28. Li, X., et al., *Sub-micrometer-scale chemical analysis by nanosecond-laser-induced tip-enhanced ablation and ionization time-of-flight mass spectrometry*. Nano Research, 2018. **11**(11): p. 5989-5996.
29. Cao, F., F. Donnarumma, and K.K. Murray, *Wavelength-Dependent Tip-Enhanced Laser Ablation of Organic Dyes*. The Journal of Physical Chemistry C, 2019. **124**(3): p. 1918-1922.
30. Nudnova, M.M., et al., *Plasma ionization source for atmospheric pressure mass spectrometry imaging using near-field optical laser ablation*. Analytical chemistry, 2015. **87**(2): p. 1323-1329.
31. Hirata, T., *Chemically assisted laser ablation ICP mass spectrometry*. Analytical chemistry, 2003. **75**(2): p. 228-233.
32. Guirado, S., et al., *Chemical analysis of archeological materials in submarine environments using laser-induced breakdown spectroscopy. On-site trials in the Mediterranean Sea*. Spectrochimica Acta Part B: Atomic Spectroscopy, 2012. **74**: p. 137-143.
33. Asmus, J., et al. *Underwater inverse LIBS (iLIBS) for marine archaeology*. in *Optics for Arts, Architecture, and Archaeology IV*. 2013. International Society for Optics and Photonics.
34. Lazic, V., J. Laserna, and S. Jovicevic, *Insights in the laser-induced breakdown spectroscopy signal generation underwater using dual pulse excitation—Part I: Vapor bubble, shockwaves and plasma*. Spectrochimica Acta Part B: Atomic Spectroscopy, 2013. **82**: p. 42-49.
35. Guo, J., et al., *Development of a compact underwater laser-induced breakdown spectroscopy (LIBS) system and preliminary results in sea trials*. Applied Optics, 2017. **56**(29): p. 8196-8200.
36. Matsumoto, A., et al., *On-site quantitative elemental analysis of metal ions in aqueous solutions by underwater laser-induced breakdown spectroscopy combined with electrodeposition under controlled potential*. Analytical chemistry, 2015. **87**(3): p. 1655-1661.
37. Matsumoto, A., et al., *A calibration-free approach for on-site multi-element analysis of metal ions in aqueous solutions by electrodeposition-assisted underwater laser-induced breakdown spectroscopy*. Spectrochimica Acta Part B: Atomic Spectroscopy, 2016. **118**: p. 45-55.
38. Jiang, T.-J., et al., *In situ underwater laser-induced breakdown spectroscopy analysis for trace Cr (VI) in aqueous solution supported by electrosorption enrichment and a gas-assisted localized liquid discharge apparatus*. Analytical chemistry, 2017. **89**(10): p. 5557-5564.
39. Goueguel, C., et al., *Resonant laser-induced breakdown spectroscopy for analysis of lead traces in copper alloys*. Journal Of Analytical Atomic Spectrometry, 2011. **26**(12): p. 2452-2460.
40. Li, Y., et al., *A review of laser-induced breakdown spectroscopy signal enhancement*. Applied Spectroscopy Reviews, 2018. **53**(1): p. 1-35.
41. Rifai, K., et al., *Resonant laser-induced breakdown spectroscopy (RLIBS) analysis of traces through selective excitation of aluminum in aluminum alloys*. Journal of Analytical Atomic Spectrometry, 2013. **28**(3): p. 388-395.

42. Frayssinous, C., et al., *Resonant polymer ablation using a compact 3.44 μm fiber laser*. Journal of Materials Processing Technology, 2018. **252**: p. 813-820.
43. Goueguel, C., et al., *Investigation of resonance-enhanced laser-induced breakdown spectroscopy for analysis of aluminium alloys*. Journal of Analytical Atomic Spectrometry, 2010. **25**(5): p. 635-644.
44. Arutyunyan, N.R., et al., *Resonant ablation of single-wall carbon nanotubes by femtosecond laser pulses*. Laser Physics, 2014. **25**(1): p. 015902.
45. Kuzema, P., *Small-molecule analysis by surface-assisted laser desorption/ionization mass spectrometry*. Journal of Analytical Chemistry, 2011. **66**(13): p. 1227-1242.
46. Murray, K.K., et al., *Definitions of terms relating to mass spectrometry (IUPAC Recommendations 2013)*. Pure and Applied Chemistry, 2013. **85**(7): p. 1515-1609.
47. Cai, Y., et al., *Multi-element analysis by ArF laser excited atomic fluorescence of laser ablated plumes: Mechanism and applications*. Frontiers of Physics, 2012. **7**(6): p. 670-678.
48. Russo, R.E., et al., *Laser ablation molecular isotopic spectrometry*. Spectrochimica Acta Part B: Atomic Spectroscopy, 2011. **66**(2): p. 99-104.
49. Bol'shakov, A.A., et al., *Laser ablation molecular isotopic spectrometry (LAMIS): current state of the art*. Journal of Analytical Atomic Spectrometry, 2016. **31**(1): p. 119-134.
50. Sturm, V., et al., *Bulk analysis of steel samples with surface scale layers by enhanced laser ablation and LIBS analysis of C, P, S, Al, Cr, Cu, Mn and Mo*. Journal of analytical atomic spectrometry, 2004. **19**(4): p. 451-456.
51. Nemes, P., et al., *Ambient molecular imaging and depth profiling of live tissue by infrared laser ablation electrospray ionization mass spectrometry*. Analytical chemistry, 2008. **80**(12): p. 4575-4582.
52. Cui, Y., et al., *Depth profiling and imaging capabilities of an ultrashort pulse laser ablation time of flight mass spectrometer*. Review of Scientific Instruments, 2012. **83**(9): p. 093702.
53. Benson, A., et al., *Laser ablation depth profiling of U-series and Sr isotopes in human fossils*. Journal of archaeological science, 2013. **40**(7): p. 2991-3000.
54. Dow, A.R., A.M. Wittig, and H.I. Kenttämä, *Laser-induced acoustic desorption mass spectrometry*. European Journal of Mass Spectrometry, 2012. **18**(2): p. 77-92.
55. Lu, I.-C., et al., *Ionization mechanism of matrix-assisted laser desorption/ionization*. Annual Review of Analytical Chemistry, 2015. **8**: p. 21-39.
56. Zenobi, R. and R. Knochenmuss, *Ion formation in MALDI mass spectrometry*. Mass spectrometry reviews, 1998. **17**(5): p. 337-366.
57. Krüger, R. and M. Karas, *Formation and fate of ion pairs during MALDI analysis: anion adduct generation as an indicative tool to determine ionization processes*. Journal of the American Society for Mass Spectrometry, 2002. **13**(10): p. 1218-1226.
58. Londero, P.S., J.R. Lombardi, and M. Leona, *Laser ablation surface-enhanced Raman microspectroscopy*. Analytical chemistry, 2013. **85**(11): p. 5463-5467.
59. Cesaratto, A., et al., *Fourier filtering ultraviolet laser ablation SERS for the analysis of yellow lakes*. Microchemical Journal, 2016. **126**: p. 237-242.
60. Bogaerts, A. and Z. Chen, *Effect of laser parameters on laser ablation and laser-induced plasma formation: A numerical modeling investigation*. Spectrochimica Acta Part B: Atomic Spectroscopy, 2005. **60**(9-10): p. 1280-1307.
61. Bogaerts, A., et al., *Laser ablation for analytical sampling: what can we learn from modeling?* Spectrochimica Acta Part B: Atomic Spectroscopy, 2003. **58**(11): p. 1867-1893.
62. Boueri, M., et al., *Early stage expansion and time-resolved spectral emission of laser-induced plasma from polymer*. Applied Surface Science, 2009. **255**(24): p. 9566-9571.
63. Yoo, J.H., et al., *Existence of phase explosion during laser ablation and its effects on inductively coupled plasma-mass spectrometry*. Analytical chemistry, 2001. **73**(10): p. 2288-2293.

64. Chen, Z. and A. Bogaerts, *Laser ablation of Cu and plume expansion into 1 atm ambient gas*. Journal of Applied Physics, 2005. **97**(6): p. 063305.
65. Bogaerts, A. and Z. Chen, *Nanosecond laser ablation of Cu: modeling of the expansion in He background gas, and comparison with expansion in vacuum*. Journal of Analytical Atomic Spectrometry, 2004. **19**(9): p. 1169-1176.
66. Gamaly, E.G., et al., *Ablation of solids by femtosecond lasers: Ablation mechanism and ablation thresholds for metals and dielectrics*. Physics of plasmas, 2002. **9**(3): p. 949-957.
67. Perry, M., et al., *Ultrashort-pulse laser machining of dielectric materials*. Journal of applied physics, 1999. **85**(9): p. 6803-6810.
68. Kramer, T., et al., *Ablation dynamics—from absorption to heat accumulation/ultra-fast laser matter interaction*. Advanced Optical Technologies, 2018. **7**(3): p. 129-144.
69. Hashida, M., et al., *Ablation threshold dependence on pulse duration for copper*. Applied surface science, 2002. **197**: p. 862-867.
70. Jaeggi, B., et al., *Laser Micromachining of Metals with Ultra-Short Pulses: Factors Limiting the Scale-Up Process*. Journal of Laser Micro/Nanoengineering, 2017. **12**(3).
71. Lauer, B., B. Jäggi, and B. Neuenschwander, *Influence of the pulse duration onto the material removal rate and machining quality for different types of steel*. Physics Procedia, 2014. **56**: p. 963-972.
72. Nolte, S., et al., *Ablation of metals by ultrashort laser pulses*. JOSA B, 1997. **14**(10): p. 2716-2722.
73. Jaeggi, B., et al. *Influence of the pulse duration and the experimental approach onto the specific removal rate for ultra-short pulses*. in *Laser Applications in Microelectronic and Optoelectronic Manufacturing (LAMOM) XXII*. 2017. International Society for Optics and Photonics.
74. Jaeggi, B., et al., *Optimizing the Specific Removal Rate with the Burst Mode Under Varying Conditions*. Journal of Laser Micro/Nanoengineering, 2017. **12**(3).
75. Shaikh, N.M., et al., *Measurement of electron density and temperature of a laser-induced zinc plasma*. Journal of physics d: applied physics, 2006. **39**(7): p. 1384.
76. Russo, R., et al., *Influence of wavelength on fractionation in laser ablation ICP-MS*. Journal of Analytical Atomic Spectrometry, 2000. **15**(9): p. 1115-1120.
77. Russo, R.E., et al., *Femtosecond laser ablation ICP-MS*. Journal of Analytical Atomic Spectrometry, 2002. **17**(9): p. 1072-1075.
78. Stolee, J.A., et al., *Laser–nanostructure interactions for ion production*. Physical Chemistry Chemical Physics, 2012. **14**(24): p. 8453-8471.
79. Olivié, G., et al., *Wavelength dependence of femtosecond laser ablation threshold of corneal stroma*. Optics express, 2008. **16**(6): p. 4121-4129.
80. LaHaye, N., et al., *The effect of ultrafast laser wavelength on ablation properties and implications on sample introduction in inductively coupled plasma mass spectrometry*. Journal of applied physics, 2013. **114**(2): p. 023103.
81. Rainer, M., M.N. Qureshi, and G.K. Bonn, *Matrix-free and material-enhanced laser desorption/ionization mass spectrometry for the analysis of low molecular weight compounds*. Analytical and bioanalytical chemistry, 2011. **400**(8): p. 2281-2288.
82. Caricato, A.P., *MAPLE and MALDI: Theory and Experiments*, in *Lasers in Materials Science*. 2014, Springer. p. 295-323.
83. Dreisewerd, K., *The desorption process in MALDI*. Chemical reviews, 2003. **103**(2): p. 395-426.
84. Dreisewerd, K., et al., *Fundamentals of matrix-assisted laser desorption/ionization mass spectrometry with pulsed infrared lasers*. International Journal of Mass Spectrometry, 2003. **226**(1): p. 189-209.

85. Feldhaus, D., et al., *Influence of the laser fluence in infrared matrix-assisted laser desorption/ionization with a 2.94  $\mu\text{m}$  Er: YAG laser and a flat-top beam profile*. Journal of mass spectrometry, 2000. **35**(11): p. 1320-1328.
86. Jackson, S.N., S. Mishra, and K.K. Murray, *On-line laser desorption/ionization mass spectrometry of matrix-coated aerosols*. Rapid communications in mass spectrometry, 2004. **18**(18): p. 2041-2045.
87. Qiao, H., V. Spicer, and W. Ens, *The effect of laser profile, fluence, and spot size on sensitivity in orthogonal-injection matrix-assisted laser desorption/ionization time-of-flight mass spectrometry*. Rapid Communications in Mass Spectrometry, 2008. **22**(18): p. 2779-2790.
88. Peterson, D.S., *Matrix-free methods for laser desorption/ionization mass spectrometry*. Mass spectrometry reviews, 2007. **26**(1): p. 19-34.
89. Silina, Y.E. and D.A. Volmer, *Nanostructured solid substrates for efficient laser desorption/ionization mass spectrometry (LDI-MS) of low molecular weight compounds*. Analyst, 2013. **138**(23): p. 7053-7065.
90. Abdelhamid, H.N. and H.-F. Wu, *Gold nanoparticles assisted laser desorption/ionization mass spectrometry and applications: from simple molecules to intact cells*. Analytical and bioanalytical chemistry, 2016. **408**(17): p. 4485-4502.
91. Picca, R.A., et al., *Mechanisms of nanophase-induced desorption in LDI-MS. A short review*. Nanomaterials, 2017. **7**(4): p. 75.
92. Link, S. and M.A. El-Sayed, *Optical properties and ultrafast dynamics of metallic nanocrystals*. Annual review of physical chemistry, 2003. **54**(1): p. 331-366.
93. Hu, M., et al., *Gold nanostructures: engineering their plasmonic properties for biomedical applications*. Chemical Society Reviews, 2006. **35**(11): p. 1084-1094.
94. Zhang, J.Z. and C. Noguez, *Plasmonic optical properties and applications of metal nanostructures*. Plasmonics, 2008. **3**(4): p. 127-150.
95. Wang, L., M. Hasanzadeh Kafshgari, and M. Meunier, *Optical Properties and Applications of Plasmonic-Metal Nanoparticles*. Advanced Functional Materials, 2020. **30**(51): p. 2005400.
96. Linic, S., P. Christopher, and D.B. Ingram, *Plasmonic-metal nanostructures for efficient conversion of solar to chemical energy*. Nature materials, 2011. **10**(12): p. 911-921.
97. Taliercio, T. and P. Biagioni, *Semiconductor infrared plasmonics*. Nanophotonics, 2019. **8**(6): p. 949-990.
98. Kriegel, I., F. Scotognella, and L. Manna, *Plasmonic doped semiconductor nanocrystals: Properties, fabrication, applications and perspectives*. Physics Reports, 2017. **674**: p. 1-52.
99. Crouch, C.H., et al., *Infrared absorption by sulfur-doped silicon formed by femtosecond laser irradiation*. Applied Physics A, 2004. **79**(7): p. 1635-1641.
100. Huang, M.H., *Facet-Dependent Optical Properties of Semiconductor Nanocrystals*. Small, 2019. **15**(7): p. 1804726.
101. Mak, K.F., et al., *Optical spectroscopy of graphene: From the far infrared to the ultraviolet*. Solid State Communications, 2012. **152**(15): p. 1341-1349.
102. Low, T. and P. Avouris, *Graphene plasmonics for terahertz to mid-infrared applications*. ACS nano, 2014. **8**(2): p. 1086-1101.
103. Ogawa, S., S. Fukushima, and M. Shimatani, *Graphene Plasmonics in Sensor Applications: A Review*. Sensors, 2020. **20**(12): p. 3563.
104. Chu, H., et al., *Recent investigations on nonlinear absorption properties of carbon nanotubes*. Nanophotonics, 2020. **9**(4): p. 761-781.
105. Mintz, K.J., Y. Zhou, and R.M. Leblanc, *Recent development of carbon quantum dots regarding their optical properties, photoluminescence mechanism, and core structure*. Nanoscale, 2019. **11**(11): p. 4634-4652.
106. Liu, M., *Optical properties of carbon dots: a review*. Nanoarchitectonics, 2020: p. 1-12.
107. Chen, Z., A. Bogaerts, and A. Vertes, *Phase explosion in atmospheric pressure infrared laser ablation from water-rich targets*. Applied Physics Letters, 2006. **89**(4): p. 041503.

108. Ionin, A.A., S.I. Kudryashov, and A.A. Samokhin, *Material surface ablation produced by ultrashort laser pulses*. Physics-Uspekhi, 2017. **60**(2): p. 149.
109. Lazic, V. and S. Jovičević, *Laser induced breakdown spectroscopy inside liquids: processes and analytical aspects*. Spectrochimica Acta Part B: Atomic Spectroscopy, 2014. **101**: p. 288-311.
110. Dharmadhikari, J., et al., *Optical control of filamentation-induced damage to DNA by intense, ultrashort, near-infrared laser pulses*. Scientific reports, 2016. **6**(1): p. 1-9.
111. Linz, N., et al., *Wavelength dependence of femtosecond laser-induced breakdown in water and implications for laser surgery*. Physical Review B, 2016. **94**(2): p. 024113.
112. Vanraes, P. and A. Bogaerts, *Plasma physics of liquids - a focused review*. Applied Physics Reviews, 2018. **5**(3): p. 031103.
113. Balling, P. and J. Schou, *Femtosecond-laser ablation dynamics of dielectrics: basics and applications for thin films*. Reports on progress in physics, 2013. **76**(3): p. 036502.
114. Mouskeftaras, A., et al., *Mechanisms of femtosecond laser ablation of dielectrics revealed by double pump-probe experiment*. Applied Physics A, 2013. **110**(3): p. 709-715.
115. Guizard, S., et al. *Femtosecond laser ablation of dielectrics: Experimental studies of fundamental processes*. in *AIP Conference Proceedings*. 2010. American Institute of Physics.
116. Nishikawa, H., et al., *Mechanism for excimer-laser ablation in alkaline-earth metals*. Physical Review B, 2000. **61**(2): p. 967.
117. Locke, B.R. and S.M. Thagard, *Analysis and review of chemical reactions and transport processes in pulsed electrical discharge plasma formed directly in liquid water*. Plasma Chemistry and Plasma Processing, 2012. **32**(5): p. 875-917.
118. Korobeinikov, S.M., A.V. Melekhov, and A.S. Besov, *Breakdown initiation in water with the aid of bubbles*. High temperature, 2002. **40**(5): p. 652-659.
119. Starikovskiy, A., et al., *Non-equilibrium plasma in liquid water: dynamics of generation and quenching*. Plasma Sources Science and Technology, 2011. **20**(2): p. 024003.
120. Shneider, M., M. Pekker, and A. Fridman, *Theoretical study of the initial stage of sub-nanosecond pulsed breakdown in liquid dielectrics*. IEEE Transactions on Dielectrics and Electrical Insulation, 2012. **19**(5): p. 1579-1582.
121. Sun, A., C. Huo, and J. Zhuang, *Formation mechanism of streamer discharges in liquids: a review*. High Voltage, 2016. **1**(2): p. 74-80.
122. Major, B., et al. *Functionally gradient materials of new generation fabricated by ablation and pulsed laser deposition*. in *Laser Technology VII: Applications of Lasers*. 2003. International Society for Optics and Photonics.
123. Bleiner, D., L. Juha, and D. Qu, *Soft X-ray laser ablation for nano-scale chemical mapping microanalysis*. Journal of Analytical Atomic Spectrometry, 2020. **35**(6): p. 1051-1070.
124. Takamizawa, A., et al., *Explosive boiling of water after pulsed IR laser heating*. Physical Chemistry Chemical Physics, 2003. **5**(5): p. 888-895.
125. Busch, K.L., *Special feature: tutorial. Desorption ionization mass spectrometry*. Journal of mass spectrometry, 1995. **30**(2): p. 233-240.
126. Chenu, A. and G.D. Scholes, *Coherence in energy transfer and photosynthesis*. Annual review of physical chemistry, 2015. **66**: p. 69-96.
127. Andrews, D.L., C. Curutchet, and G.D. Scholes, *Resonance energy transfer: beyond the limits*. Laser & Photonics Reviews, 2011. **5**(1): p. 114-123.
128. Morresi, A., et al., *Vibrational relaxation processes in isotropic molecular liquids. A critical comparison*. Journal of Raman Spectroscopy, 1995. **26**(3): p. 179-216.
129. Fabian, J. and P.B. Allen, *Anharmonic decay of vibrational states in amorphous silicon*. Physical review letters, 1996. **77**(18): p. 3839.
130. Bolmatov, D., V. Brazhkin, and K. Trachenko, *The phonon theory of liquid thermodynamics*. Scientific reports, 2012. **2**: p. 421.
131. Bolmatov, D., et al., *Unified phonon-based approach to the thermodynamics of solid, liquid and gas states*. Annals of Physics, 2015. **363**: p. 221-242.

132. Brazhkin, V. and K. Trachenko, *Between glass and gas: Thermodynamics of liquid matter*. Journal of Non-Crystalline Solids, 2015. **407**: p. 149-153.
133. Kammann, E., et al., *Crossover from photon to exciton-polariton lasing*. New Journal of Physics, 2012. **14**(10): p. 105003.
134. Zhang, C., et al., *Two-photon pumped lasing in single-crystal organic nanowire exciton polariton resonators*. Journal of the American Chemical Society, 2011. **133**(19): p. 7276-7279.
135. Berini, P. and I. De Leon, *Surface plasmon-polariton amplifiers and lasers*. Nature photonics, 2012. **6**(1): p. 16-24.
136. Bozhevolnyi, S.I., et al., *Channel plasmon-polariton guiding by subwavelength metal grooves*. Physical review letters, 2005. **95**(4): p. 046802.
137. Jacob, Z., *Nanophotonics: hyperbolic phonon-polaritons*. Nature materials, 2014. **13**(12): p. 1081-1083.
138. Razdolski, I., et al., *Second harmonic generation from strongly coupled localized and propagating phonon-polariton modes*. Physical Review B, 2018. **98**(12): p. 125425.
139. Giret, Y., et al., *Nonthermal solid-to-solid phase transitions in tungsten*. Physical Review B, 2014. **90**(9): p. 094103.
140. Dorchie, F. and V. Recoules, *Non-equilibrium solid-to-plasma transition dynamics using XANES diagnostic*. Physics Reports, 2016. **657**: p. 1-26.
141. Rethfeld, B., et al., *Modelling ultrafast laser ablation*. Journal of Physics D: Applied Physics, 2017. **50**(19): p. 193001.
142. Sundaram, S. and E. Mazur, *Inducing and probing non-thermal transitions in semiconductors using femtosecond laser pulses*. Nature materials, 2002. **1**(4): p. 217.
143. Yang, G., *Laser ablation in liquids: principles and applications in the preparation of nanomaterials*. 2012: CRC Press.
144. Sugioka, K., M. Meunier, and A. Piqué, *Laser precision microfabrication*. Vol. 135. 2010: Springer.
145. Weber, S.T. and B. Rethfeld, *Phonon-induced long-lasting nonequilibrium in the electron system of a laser-excited solid*. Physical Review B, 2019. **99**(17): p. 174314.
146. Klett, I. and B. Rethfeld, *Relaxation of a nonequilibrium phonon distribution induced by femtosecond laser irradiation*. Physical Review B, 2018. **98**(14): p. 144306.
147. Callan, J.P., *Ultrafast dynamics and phase changes in solids excited by femtosecond laser pulses*, in *Ph.D. Thesis*. 2000. p. 2604.
148. Anisimov, S., B. Kapeliovich, and T. Perelman, *Electron emission from metal surfaces exposed to ultrashort laser pulses*. Zh. Eksp. Teor. Fiz, 1974. **66**(2): p. 375-377.
149. Anisimov, S.I., *Effect of the powerful light fluxes on metals*. Sov. Phys. Tech. Phys., 1967. **11**: p. 945.
150. Ivanov, D.S. and L.V. Zhigilei, *Combined atomistic-continuum modeling of short-pulse laser melting and disintegration of metal films*. Physical Review B, 2003. **68**(6): p. 064114.
151. Norman, G., et al., *Nanomodification of gold surface by picosecond soft x-ray laser pulse*. Journal of Applied Physics, 2012. **112**(1): p. 013104.
152. Gill-Comeau, M. and L.J. Lewis, *Ultrashort-pulse laser ablation of nanocrystalline aluminum*. Physical Review B, 2011. **84**(22): p. 224110.
153. Demaske, B.J., et al., *Ablation and spallation of gold films irradiated by ultrashort laser pulses*. Physical Review B, 2010. **82**(6): p. 064113.
154. Upadhyay, A.K., et al., *Ablation by ultrashort laser pulses: Atomistic and thermodynamic analysis of the processes at the ablation threshold*. Physical Review B, 2008. **78**(4): p. 045437.
155. Wu, C., et al., *Runaway lattice-mismatched interface in an atomistic simulation of femtosecond laser irradiation of Ag film-Cu substrate system*. Applied Physics A, 2011. **104**(3): p. 781-792.

156. Karim, E.T., Z. Lin, and L.V. Zhigilei. *Molecular dynamics study of femtosecond laser interactions with Cr targets*. in *AIP Conference Proceedings*. 2012. American Institute of Physics.
157. Zhigilei, L.V., Z. Lin, and D.S. Ivanov, *Atomistic modeling of short pulse laser ablation of metals: connections between melting, spallation, and phase explosion*. *The Journal of Physical Chemistry C*, 2009. **113**(27): p. 11892-11906.
158. Caruso, F., et al., *Electron-plasmon and electron-phonon satellites in the angle-resolved photoelectron spectra of n-doped anatase TiO<sub>2</sub>*. *Physical Review B*, 2018. **97**(16): p. 165113.
159. Tohidi, M., et al., *Modelling Low Field Electron Mobility In Group III Nitride Materials*. *International Journal of Engineering Research and Applications*, 2013. **3**(4).
160. Kong, J., et al., *Hot electron plasmon-protected solar cell*. *Optics express*, 2015. **23**(19): p. A1087-A1095.
161. Wang, Z., et al., *Thermoelectric transport properties of silicon: Toward an ab initio approach*. *Physical Review B*, 2011. **83**(20): p. 205208.
162. Dulkeith, E., et al., *Plasmon emission in photoexcited gold nanoparticles*. *Physical Review B*, 2004. **70**(20): p. 205424.
163. Van der Mullen, J., *Excitation equilibria in plasmas; a classification*. *Physics Reports*, 1990. **191**(2-3): p. 109-220.
164. Chang, T.C. and D.D. Dlott, *Vibrational cooling in large molecular systems: Pentacene in naphthalene*. *The Journal of Chemical Physics*, 1989. **90**(7): p. 3590-3602.
165. Kim, H. and D.D. Dlott, *Theory of ultrahot molecular solids: Vibrational cooling and shock-induced multiphonon up pumping in crystalline naphthalene*. *The Journal of Chemical Physics*, 1990. **93**(3): p. 1695-1709.
166. Ahmed, N., S. Darwish, and A.M. Alahmari, *Laser ablation and laser-hybrid ablation processes: a review*. *Materials and Manufacturing Processes*, 2016. **31**(9): p. 1121-1142.
167. Reif, J., et al. *The role of asymmetric excitation in self-organized nanostructure formation upon femtosecond laser ablation*. in *AIP Conference Proceedings*. 2012. American Institute of Physics.
168. Yuan, Y., et al., *Simulation of rippled structure adjustments based on localized transient electron dynamics control by femtosecond laser pulse trains*. *Applied Physics A*, 2013. **111**(3): p. 813-819.
169. Miyaji, G. and K. Miyazaki, *Origin of periodicity in nanostructuring on thin film surfaces ablated with femtosecond laser pulses*. *Optics express*, 2008. **16**(20): p. 16265-16271.
170. Joshi, A. and A. Majumdar, *Transient ballistic and diffusive phonon heat transport in thin films*. *Journal of Applied Physics*, 1993. **74**(1): p. 31-39.
171. Leveugle, E., D.S. Ivanov, and L.V. Zhigilei, *Photomechanical spallation of molecular and metal targets: molecular dynamics study*. *Applied Physics A*, 2004. **79**(7): p. 1643-1655.
172. Zhigilei, L.V. and B.J. Garrison, *Microscopic mechanisms of laser ablation of organic solids in the thermal and stress confinement irradiation regimes*. *Journal of Applied Physics*, 2000. **88**(3): p. 1281-1298.
173. Chichkov, B.N., et al., *Femtosecond, picosecond and nanosecond laser ablation of solids*. *Applied physics A*, 1996. **63**(2): p. 109-115.
174. Yilbas, B., et al., *Laser-shock processing of steel*. *Journal of Materials Processing Technology*, 2003. **135**(1): p. 6-17.
175. Zeng, X., et al., *Experimental investigation of ablation efficiency and plasma expansion during femtosecond and nanosecond laser ablation of silicon*. *Applied Physics A*, 2005. **80**(2): p. 237-241.
176. König, J., S. Nolte, and A. Tünnermann, *Plasma evolution during metal ablation with ultrashort laser pulses*. *Optics Express*, 2005. **13**(26): p. 10597-10607.
177. Liu, C., et al., *Nanosecond and femtosecond laser ablation of brass: particulate and ICPMS measurements*. *Analytical Chemistry*, 2004. **76**(2): p. 379-383.

178. Lu, Q., et al., *Delayed phase explosion during high-power nanosecond laser ablation of silicon*. Applied physics letters, 2002. **80**(17): p. 3072-3074.
179. Lu, Q., et al., *Theory analysis of wavelength dependence of laser-induced phase explosion of silicon*. Journal of Applied Physics, 2008. **104**(8): p. 083301.
180. Lee, Y., et al., *Spatial and temporal distribution of metal atoms and their diatomic oxide molecules in femtosecond laser-induced plasmas*. Journal of Analytical Atomic Spectrometry, 2018. **33**(11): p. 1875-1883.
181. Verhoff, B., S. Harilal, and A. Hassanein, *Angular emission of ions and mass deposition from femtosecond and nanosecond laser-produced plasmas*. Journal of Applied Physics, 2012. **111**(12): p. 123304.
182. Anoop, K., et al., *Two-dimensional imaging of atomic and nanoparticle components in copper plasma plume produced by ultrafast laser ablation*. Applied Physics A, 2014. **117**(1): p. 313-318.
183. Miloshevsky, A., et al., *Generation of nanoclusters by ultrafast laser ablation of Al: Molecular dynamics study*. Physical Review Materials, 2017. **1**(6): p. 063602.
184. Teghil, R., et al., *Picosecond and femtosecond pulsed laser ablation and deposition of quasicrystals*. Applied Surface Science, 2003. **210**(3-4): p. 307-317.
185. Gurevich, E. and R. Hergenröder, *Femtosecond laser-induced breakdown spectroscopy: physics, applications, and perspectives*. Applied spectroscopy, 2007. **61**(10): p. 233A-242A.
186. Harilal, S., *Influence of spot size on propagation dynamics of laser-produced tin plasma*. Journal of Applied Physics, 2007. **102**(12): p. 123306.
187. Russo, R.E., et al., *Laser ablation in analytical chemistry*. 2013, ACS Publications.
188. Poitrasson, F., et al., *Comparison of ultraviolet femtosecond and nanosecond laser ablation inductively coupled plasma mass spectrometry analysis in glass, monazite, and zircon*. Analytical Chemistry, 2003. **75**(22): p. 6184-6190.
189. Gamaly, E.G. and A.V. Rode, *Physics of ultra-short laser interaction with matter: From phonon excitation to ultimate transformations*. Progress in Quantum Electronics, 2013. **37**(5): p. 215-323.
190. Verdun, F., G. Krier, and J. Muller, *Increased sensitivity in laser microprobe mass analysis by using resonant two-photon ionization processes*. Analytical Chemistry, 1987. **59**(10): p. 1383-1387.
191. Zhang, C., et al., *One-dimensional transient analysis of volumetric heating for laser drilling*. Journal of applied physics, 2006. **99**(11): p. 113530.
192. Yonezawa, T., et al., *Detailed investigation on the possibility of nanoparticles of various metal elements for surface-assisted laser desorption/ionization mass spectrometry*. Analytical Sciences, 2009. **25**(3): p. 339-346.
193. Tang, H.-W., et al., *Ion desorption efficiency and internal energy transfer in carbon-based surface-assisted laser desorption/ionization mass spectrometry: desorption mechanism (s) and the design of SALDI substrates*. Analytical chemistry, 2009. **81**(12): p. 4720-4729.
194. Silina, Y.E., M. Koch, and D.A. Volmer, *Influence of surface melting effects and availability of reagent ions on LDI-MS efficiency after UV laser irradiation of Pd nanostructures*. Journal of Mass Spectrometry, 2015. **50**(3): p. 578-585.
195. Ng, K.-M., et al., *Ion-desorption efficiency and internal-energy transfer in surface-assisted laser desorption/ionization: more implication (s) for the thermal-driven and phase-transition-driven desorption process*. The Journal of Physical Chemistry C, 2015. **119**(41): p. 23708-23720.
196. Kurita, M., R. Arakawa, and H. Kawasaki, *Silver nanoparticle functionalized glass fibers for combined surface-enhanced Raman scattering spectroscopy (SERS)/surface-assisted laser desorption/ionization (SALDI) mass spectrometry via plasmonic/thermal hot spots*. Analyst, 2016. **141**(20): p. 5835-5841.

197. Lai, S.K.-M., et al., *Nanosecond UV Laser Ablation of Gold Nanoparticles: Enhancement of Ion Desorption by Thermal-Driven Desorption, Vaporization, or Phase Explosion*. The Journal of Physical Chemistry C, 2016. **120**(36): p. 20368-20377.
198. Karas, M. and R. Krüger, *Ion formation in MALDI: the cluster ionization mechanism*. Chemical reviews, 2003. **103**(2): p. 427-440.
199. Mao, S.S., et al., *Initiation of an early-stage plasma during picosecond laser ablation of solids*. Applied Physics Letters, 2000. **77**(16): p. 2464-2466.
200. Huang, M.-Z., et al., *Ambient ionization mass spectrometry: a tutorial*. Analytica chimica acta, 2011. **702**(1): p. 1-15.
201. Mao, X.L., et al., *Temperature and emission spatial profiles of laser-induced plasmas during ablation using time-integrated emission spectroscopy*. Applied Spectroscopy, 1995. **49**(7): p. 1054-1062.
202. Bulgakova, N., et al. *Charging and plasma effects under ultrashort pulsed laser ablation*. in *High-Power Laser Ablation VII*. 2008. International Society for Optics and Photonics.
203. Knochenmuss, R. and R. Zenobi, *MALDI ionization: the role of in-plume processes*. Chemical reviews, 2003. **103**(2): p. 441-452.
204. He, H., et al., *Recent advances in nanostructure/nanomaterial-assisted laser desorption/ionization mass spectrometry of low molecular mass compounds*. Analytica chimica acta, 2019. **1090**: p. 1-22.
205. Sandhu, A.S., et al., *Laser-generated ultrashort multimegagauss magnetic pulses in plasmas*. Physical review letters, 2002. **89**(22): p. 225002.
206. Schumaker, W., et al., *Ultrafast electron radiography of magnetic fields in high-intensity laser-solid interactions*. Physical review letters, 2013. **110**(1): p. 015003.
207. Tatarakis, M., et al., *Measuring huge magnetic fields*. Nature, 2002. **415**(6869): p. 280-280.
208. Khan, M., et al., *Self-generated magnetic field and Faraday rotation in a laser-produced plasma*. Physical Review E, 1998. **58**(1): p. 925.
209. Liu, S. and X. Li, *Numerical analysis of self-generated magnetic field excited by transverse plasmons in a laser-produced plasma*. Journal of plasma physics, 2001. **66**(4): p. 223-238.
210. Albertazzi, B., et al., *Dynamics and structure of self-generated magnetic fields on solids following high contrast, high intensity laser irradiation*. Physics of Plasmas, 2015. **22**(12): p. 123108.
211. Kuri, D.K., N. Das, and K. Patel, *Formation of periodic magnetic field structures in overdense plasmas*. Laser and Particle Beams, 2017. **35**(3): p. 467-475.